California Institute of Technology

W. M. Keck Laboratory of Engineering Materials

DISLOCATION VELOCITY MEASUREMENTS

by

T. Vreeland, Jr.

A Chapter Contributed to the Series

"TECHNIQUES IN METALS RESEARCH"

R. F. Bunshah, Editor

John Wiley & Sons, Inc.

Submitted to the U. S. Atomic Energy Commission
under Contract # AT(04-3)-473

January 1967

DISLOCATION VELOCITY MEASUREMENTS*

T. Vreeland, Jr.

W. M. Keck Laboratory of Engineering Materials
California Institute of Technology, Pasadena

Measurement of dislocation velocities requires the use of many of the techniques described in the foregoing chapters. In addition, special systems for applying controlled, short-duration velocities in excess of several mm/sec. The application of these techniques to the measurement of dislocation velocity is the subject of this chapter.

I. The Significance of Dislocation Velocity

The velocity of dislocations in crystals is of interest because of the direct dependence of plastic strain rate on dislocation velocity. This dependence is due to the fact that dislocation motion results in plastic deformation as expressed by the relation

$$\gamma_p = Ab/V = A_o b \qquad (1)$$

where γ_p is the plastic shear strain resulting from dislocations of strength b, sweeping out a total slip plane area of A in a crystal of volume V (A_o is then the area per unit volume swept out by the dislocations). Equation 1 relates a macroscipic quantity (plastic shear strain) to the microscopic dislocation parameters A_o and b for the case of simple shear. More complex expressions may be obtained relating the macroscopic quantities of lattice curvature and twist to the microscopic

* Portions of the work reported herein were supported by the U. S. Atomic Energy Commission under Contract No. AT(04-3)-473.

dislocation parameters. Differentiation of these expressions with respect to time gives the rate of plastic deformation, and for simple shear we find

$$\dot{\gamma}_p = \dot{A}_o b = b\int v dl \qquad (2)$$

where v is the velocity of an element dl of dislocation line, and the integral is taken over all of the dislocations in a unit volume. If we replace the integral in equation 2 by the average velocity $\bar{v}$ times the length of dislocation line per unit volume ρ there results the well-known relation

$$\dot{\gamma}_p = \rho b \bar{v} \qquad (3)$$

The length of dislocation per unit volume, or dislocation density, can be taken to be the total length per unit volume ρ_t, but it is generally somewhat easier to describe $\bar{v}$ if we take ρ to be the density of <u>moving</u> dislocations, ρ_m.

The essential assumptions used in relating the plastic strain rate to the product of moving dislocation density and average dislocation velocity are:

1) Plastic flow occurs by the motion of dislocations, and
2) The dislocation motion occurs in such a manner that an average value of dislocation velocity exists.

Equation 3, which relates the macroscopic shear strain rate to the dislocation density, dislocation strength, and dislocation velocity, may be extended to the case wherein slip on different slip systems is occurring simultaneously to produce plastic extension or contraction. The contribution to the total deformation rate from slip on a given slip system is proportional to the product of the moving dislocation density, the dislocation strength, and the average dislocation velocity on that system. In

materials which deform inhomogeneously by the formation and growth of slip bands, the rate of slip band growth, the number of bands, and the dislocation density in the bands determine the macroscopic strain rate. Gilman has pointed out that the description of plastic deformation in terms of dislocation mechanics represents a significant advance over classical plasticity theory.[1] When the parameters $\bar{v}$ and ρ can be described as functions of the applied stress and the instantaneous strain, the macroscopic plastic strain rates can then be related to the macroscopic stress and strain. This relation permits the response of the crystal to be predicted for any load-time history, or alternately, it permits calculation of the loads required to deform a crystal on a given path of strain vs. time.

Application of the dislocation dynamics description of plastic deformation has been made to predict the dynamic stress-strain response of a crystal,[2] to describe transient creep behavior,[3] and to explain some observations in high velocity impact experiments,[4] none of which could be adequately predicted by the classical plasticity theories.

In addition to providing information useful for the prediction of material behavior, measurement of dislocation velocity gives us some direct information which relates to the dynamic interactions of the moving dislocations with the crystal lattice, with other dislocations, and with other crystal defects. For these reasons, the measurement of dislocation velocity or dislocation mobility has been undertaken by a number of investigators.

II. Some Variables which Affect the Dislocation Velocity

A. The Inertia of a Dislocation

F. C. Frank[5] has shown that the total energy per unit length of a straight screw dislocation moving at a uniform velocity v in an isotropic continuum is given by

$$U = U_o (1 - v^2/c^2)^{-1/2} \tag{4}$$

where U_o is the energy of the stationary dislocation and c is the shear wave velocity. The total energy is seen to approach infinity as v approaches c, analogous to the way in which the energy of a particle approaches infinity as its velocity approaches the speed of light. The shear wave velocity should then be an upper limit for the velocity of a screw dislocation, and this is also true in a discreet lattice according to Thompson.[6]

At velocities much less than c, the total energy per unit length of dislocation may be written as

$$U \approx U_o (1 + 1/2\ v^2/c^2) = U_o + 1/2(U_o/c^2)v^2 \tag{5}$$

The last term in equation 5 represents the kinetic energy, and from it, we deduce that the effective mass per unit length of dislocation is U_o/c^2. With $U_o \approx Gb^2$ and $c^2 = G/m_o$ where G is the shear modulus, and m_o is the mass density, the mass per unit length of dislocation is

$$U_o/c^2 \approx m_o b^2 \tag{6}$$

This is equivalent to the mass of a unit length of a cylinder of material with a diameter of the order of b.

Eshelby[7] has shown that the total energy of edge dislocations increases in a similar manner as their velocity approaches that of shear waves, and the equivalent mass of an edge oriented dislocation is then of the order of $m_o b^2$. If no energy dissipation occurs as a dislocation moves through a crystal, very high dislocation accelerations would result from application of stresses equal to the flow stress of the softest crystals. The small mass per unit length of the dislocation gives rise to appreciable inertia forces only at very large accelerations. For example, at a constant stress of 5 gm/mm^2, the acceleration of a dislocation in copper would be of the order of 10^{12} cm/sec^2, and a velocity of 10^3 cm/sec would be reached in 1 nsec with only inertia forces limiting its velocity. Experimental observations of dislocation motion over distances large compared to b have shown that there is a rapid acceleration to a terminal velocity under constant stress. The acceleration is too rapid to measure by use of currently available techniques, so we may conclude that inertia forces are relatively unimportant in limiting the dislocation velocity. The terminal velocity is a function of stress, and it has been observed to approach c at high stress in some crystals as will be shown in section IV.

B. Other Variables

The terminal velocity of a dislocation is reached when the driving force due to the applied stress is balanced by forces opposing the motion of the dislocation. The forces opposing the motion of the dislocation can come from the lattice itself, or from imperfections in the lattice.

All factors which influence the strain rate of a crystal deforming by slip must do so by their influence on the dislocation velocity and on the density of moving dislocations. It has been mentioned that the dislocation velocity is a function of stress. Other variables which are of importance are: crystal structure and bonding, temperature, impurity and other point defect concentration and distribution, and dislocation density and distribution. The velocity of a given segment of dislocation line can also be influenced by such variables as the orientation of the line with respect to the Burgers vector, the path of the segment (glissile vs. climb motion), and details of the dislocation core such as its width and its possible dissociation into partial dislocations. Our present understanding of the effect of these variables does not permit quantitative prediction of the dislocation velocity and even the relative importance of many of the variables is unknown. This situation indicates the need for measurements of dislocation velocity under conditions wherein the variables which affect the velocity are carefully controlled.

III. Considerations in the Direct Measurement of Dislocation Velocity

A. Suitable Techniques of Dislocation Observations

1. Continuous Observation

The ideal method of obtaining dislocation velocities would be to continuously observe the dislocation positions as a function of time while systematically changing the variables to quantitatively determine their effect. The techniques available for dislocation observation

limit our ability to employ such an ideal method. While the electron microscope permits continuous observation of moving dislocations in thin films, the velocities which can be observed are limited to low values, and the desired control of many of the variables is exceedingly difficult to achieve. However, pertinent observations pertaining to dislocation motion may be made due to the relatively high resolution obtainable, and the ease with which the Burgers vector of a dislocation can be determined. In experiments wherein a specimen is strained in the microscope, it is possible to observe whether the motion is continuous (within the limits of resolution obtainable) or intermittent. Obstacles such as precipitates or dislocation interactions which tend to decrease $\bar{v}$ can often be recognized because the motion is observed continuously. Quantitative dislocation velocity measurements in the electron microscope must await development of means for controlling the stress in the thin, electron transparent films.

Continuous observation of arrays of moving dislocations have been made. For example, measurements of the velocity of Lüder's bands,[8] twins,[9] and small angle grain boundaries[10,11] were made before measurements of the velocity of individual dislocations. The stress concentrations associated with Lüder's bands and twins make it difficult to deduce individual dislocation velocities as a function of stress from these measurements, and the behavior of small angle boundaries is considerably different from the behavior of isolated dislocations. Observation of thermal etching of slowly moving dislocations[12] indicates that under

special conditions, low velocity dislocations may be continuously observed by etching. This technique has not been employed for quantitative dislocation velocity measurements.

2. Intermittent Observations

a. General Considerations

While observational techniques suitable only to stationary dislocations do not permit a truly direct determination of dislocation velocity, these techniques can be used to deduce average dislocation velocity under carefully controlled conditions. When the dislocation positions before and after application of a controlled stress to the crystal are used together with the stress duration to deduce average dislocation velocities, the following considerations become important:

(1) The possibility of losing a one-to-one correspondence of dislocation positions before and after the controlled stressing. This consideration places a limitation on the dislocation displacement that can be measured, a limit which is generally equal to the initial dislocation spacing, or the diameter of the subgrains, but in special cases it may be the specimen dimensions. This is turn places an upper limit on the duration of the applied stress for a given average dislocation velocity. The strain (or dislocation density) dependence of dislocation velocity is therefore very difficult to measure directly and dislocation velocities in plastically deformed crystals with high dislocation densities have not been measured due to this limitation.

(2) The possibility of dislocation motion due to handling stresses, thermal stresses, or relaxation of internal stresses

before or after application of the controlled stress. This consideration dictates considerable care in the handling of soft crystals, but it may also limit the methods of dislocation observation that can be employed for a given crystal.

(3) The need to apply a controlled stress vs. time history so that the stress dependence can be deduced. This consideration will be discussed in section II B.

b. Use of the Etch Pit Technique

The etch pit technique has been widely used for dislocation velocity measurements. Its principle advantages are that it does not require complex equipment, it can be applied to large as well as small crystal specimens, and it does not generally require sectioning of the specimen. Many dislocation etches are only effective on surfaces oriented within a few degrees of a low index crystallographic plane. This places a condition on the geometry and orientation of the test specimens in addition to those conditions imposed by the loading system and the slip system under study. Examples of the successful application of orientation sensitive dislocation etches to the measurement of dislocation velocity are given in section IV. The "double etch" technique which reveals the previous as well as present dislocation positions is of particulat help in determination of the displacement of individual dislocations.

Slip band growth may be observed intermittently by dislocation etching. Such measurements are of importance because the rate of slip band growth is directly related to the macroscipic strain rate as indicated in

section I. Interpretation of these measurements in terms of the stress dependence of isolated dislocations is complicated by the stress concentration at the head of the slip band. The deformation pattern associated with the slip bands is sufficiently distinct to be seen in crystals of relatively high dislocation density. Such measurements can be made under conditions where the velocity of isolated dislocations cannot be obtained.

Etching in depth, to determine the shape of slip bands, will show the relative rates of motion of dislocations of different orientation. Differences in the velocity of edge and screw oriented dislocations can be observed in this manner.[13]

Dislocation etches for some materials require that impurities be concentrated at the dislocation sites. When the dislocations in these materials are displaced at velocities greater than that of the impurity drift, an aging treatment must be used to allow the impurities to segregate to the "fresh" or displaced dislocations before their positions can be determined by etching. It must be demonstrated that the aging treatments do not permit significant dislocation rearrangement before the technique is applied to dislocation velocity measurements.

The impurities in the lattice will in general influence the dislocation velocity, and in some cases impurities segregated to the dislocations will make them immobile at stresses where dislocations free of segregated impurities can move. Intentional surface damage may then be used to produce fresh dislocations, and the velocity measurements made before sufficient impurities can segregate to these dislocations to immobilize them.

One disadvantage of the etch pit technique is that the dislocation orientation cannot in general be determined from observation of an etched surface (etching in depth is required, and the possibility of climb or glide during the etching must be considered).

c. Use of X-Ray Micrography

The Berg-Barrett X-ray micrography technique (surface reflection) permits dislocation positions to be determined when the dislocations lie within several microns of the surface. Stringent requirements are placed on the orientation of the crystal with respect to the X-ray beam in order to obtain good resolution with this technique. When the slip system under study is parallel to the observation surface, experiments may be made at relatively high dislocation densities due to the limited penetration depth of the X-rays. Further, the orientation of the dislocations with respect to their Burgers vector may be readily determined. It is difficult to apply large shear stresses on a slip plane parallel to and within a few microns of the surface of a crystal. Bonding agents strong enough to transmit shear stresses of sufficient magnitudes to produce appreciable dislocation velocities exist for soft crystals, and an example of their use is given in section IV. Sectioning of relatively hard crystals to reveal a slip surface, followed by polishing to remove the cutting damage, may permit a study of dislocation motion from surface sources. The relatively long exposure times required to obtain the X-ray micrograph may be a limiting factor im some materials. An example of the use of the Berg-Barrett technique in dislocation velocity measurements is described in section IV.

The Lang and Borrmann techniques (X-ray transmission through the crystal) permit dislocations to be observed in thin crystals of low dislocation density. An example of the use of the Lang technique in dislocation velocity measurement is given in section IV.

B. Application of Controlled Stresses

1. The Stress State

The glide force per unit length of dislocation which acts perpendicular to the dislocation line is equal to $\tau_r b$ where τ_r is the resolved shear stress on the glide plane in the direction of the Burgers vector of the dislocation. The glide force is affected by internal stresses as well as the stresses resulting from applied loads. If the dislocation velocity is not <u>linearly</u> dependent on τ_r, internal stresses which have a mean value equal to zero affect the average dislocation velocity under a constant applied stress,[14] so that $\bar{v}$ is a function of both the internal stress and the applied stress.

A uniaxial state of stress is relatively easy to apply by tension, compression, or pure bending of prismatic rods (four point bending). The simplicity of this stress state and the relative ease of its control make it the first state to consider for dislocation velocity measurements. The specimen orientation with respect to the stress axis then governs the relative magnitude of the applied resolved shear stress on the various slip systems. The applied resolved shear stress is given by

$$(\tau_r)_a = \sigma \sin \chi_o \cos$$

where σ is the uniaxial stress,

χ_o is the complement of the angle between the normal to the slip plane and the stress axis, and

is the angle between the Burgers vector and the stress axis. ($\sin \chi_o \cos$ is the Schmid factor for the slip system).

Examples of the crystal orientation with respect to the uniaxial stress used by a number of investigators are given in section IV.

A uniaxial stress is obtained on the top and bottom surfaces of a simply supported beam of rectangular cross section loaded at its center (three point bending). The gradient in $\underline{\sigma}$ along the length of the beam is advantageous, as a single loading will produce stresses which vary linearly from zero at the supports to a maximum under the load. When the plastic strains produced by dislocation motion are small compared to the elastic strains, the elementary stress solutions for elastic beams can be used to relate $\underline{\sigma}$ to the beam dimensions and the applied load.

Another relatively simple state of stress useful for making measurements of dislocation velocity is that of pure shear. Torsion of a cylinder that has a twofold axis of crystallographic symmetry (or its equivalent) produces a state of pure shear. A system for the dynamic application of torsion is described in section 6, below.

Crystals in the form of plates or beams may be stressed by deforming them to known radii of curvature. The resulting elastic stresses can be calculated from anisotropic elasticity theory.[15] This stressing method appears useful for long duration tests.

2. The Application of Stress Pulses Using Conventional Loading Systems

A rectangular stress pulse of controlled stress amplitude and duration is optimum for determination of dislocation velocity when dislocation positions before and after application of the stress pulse

are determined. When the rise and fall times of the stress are small compared to the duration of the pulse, the average dislocation velocity associated with the known stress amplitude of the pulse is obtained. When the stress amplitude is not constant, determination of the stress dependence of dislocation velocity is considerably more complicated. Essentially rectangular stress pulses of duration greater than about 10 sec can be applied using manual control in conventional testing equipment. Velocities up to about 10^{-1} cm/sec can then be determined if dislocation displacements of the order of 1 cm occur. Stress overshoot is difficult to prevent when rise times less than 1 sec are achieved using manual control. Closed-loop feedback control of the application of stress in commercially available screw driven or hydraulic loading systems permits rise times of the order of 0.1 sec to be achieved without overshoot, so velocities up to approximately one cm/sec can be measured. The inertia, characteristic of the loading systems of these testing machines, prevents appreciably faster rise times without overshoot.

3. Special Rapid Loading Systems

Special loading means for more rapid application of stress may be divided into two categories according to whether or not they employ propagating wave fronts in the specimen. Stress pulses obtained by the passage of wave fronts through the crystal are discussed in the next section. When the rise time of the stress pulse is large compared to the time for stress waves to traverse the specimen, the stress will be in phase with the applied loads. Excitation of stress waves or of normal modes of vibration of the specimen is then avoided. A single rectangular

stress pulse can be applied to a crystal when the rise time of the pulse is a small fraction of the period associated with its lowest normal mode of vibration (typically one tenth or less). The periods of the fundamental bending modes of a specimen are larger than those of the longitudinal modes, so that shorter rise times can be tolerated in tension or compression than in bending.

Special loading systems have been designed to rapidly apply a load to a specimen without appreciable overshoot. This is achieved by providing for the appropriate amount of damping, as dictated by the spring rate and inertia of the specimen and loading system. Johnston and Gilman employed a four point bending jig loaded with a magnetic pulsing machine to produce short duration stress pulses.[16] This machine is shown schematically in Fig. 1a. A large electromagnet with a small, oil damped coil mounted in the magnetic gap produces a stress pulse such as that shown in Fig. 1b, when a square current pulse is passed through the coil. A rapid loading system which applies stress pulses as short as 17 msec in duration, with a rise time of 2 msec is currently being used in dislocation velocity studies at the California Institute of Technology. This system is patterned after the pneumatic-hydraulic machine described by Clark and Wood.[17] Dislocation velocities up to approximately 50 cm/sec can be measured using this system when dislocation displacements of about 1 cm are produced.

4. Stress Pulses and Propagating Waves

Stress pulses of sufficiently short duration for use in the measurement of near-sonic dislocation velocities are obtained by the

use of propagating waves. Systems which employ impact, the sudden release of elastic energy, and the detonation of an explosive to generate the stress waves are discussed below.

A rectangular stress pulse is obtained by the passage of an elastic loading wave of constant stress amplitude through a specimen, followed by an unloading wave. Non-dispersive wave fronts are desirable for the generation of stress pulses. They may be generated and measured in elastic bars and then passed through a test crystal, or they may be generated in the crystal itself. When the wave fronts are passed through interfaces between an elastic bar and the crystal, wave reflections must be avoided or elastic waves will be trapped in the crystal, and a single stress pulse cannot be obtained. Wave reflections can be avoided if the specimen remains essentially elastic, and the acoustic impedance of the specimen matches that of the elastic bar.[18] An example of impedance matching for torsional waves is given below. Non-dispersive longitudinal waves in rods are obtained when the length of the wave front along the bar is greater than several bar diameters. This dictates a minimum rise time of about 5 μsec in a steel bar one cm in diameter for a non-dispersive wave. Shorter wave lengths excite radial vibrations in the rod and dispersion results. Wave dispersion can also occur due to elastic anisotropy of the crystal. Crystal orientations with respect to the wave front should be chosen which eliminate or minimize this effect. The dislocation displacements induced by the stress pulse must give rise to plastic strains which are small compared to the elastic strains associated with the pulse if dispersion is to be avoided. Thus, only a low density of moving dislocations can be tolerated when the dislocation velocity is large.

5. Stress Pulses Generated by Impact

The rise time of a stress wave generated by the axial impact of bars is a function of the curvature of the impacting surfaces. The curvatures may be adjusted to give a sufficiently long rise time that the stress wave generated is non-dispersive.

Johnston and Gilman[16] employed an impact of a 1/16 in. diameter ball bearing on a hard steel rod to generate short compressional stress pulses. Figure 2a shows a schematic drawing of their system. A CO_2 pellet gun was used to fire the ball through four baffle plates which prevented the gas blast from reaching the bar assembly consisting of a hard steel bar, the test crystal, a thin barium titanate transducer, and a long lead bar. The lead bar was used to absorb the energy in the pulse to reduce the amplitude of pulse reflections which pass through the specimen. The bar assembly was glued together and supported as a ballistic pendulum. The shape of the stress pulse in the specimen was assumed to correspond to that measured by the barium titanate transducer. Measurement of the ballistic impulse permitted the stress amplitude to be determined. The main pulse and a smaller reflected pulse are shown in Fig. 2b. Such a short duration compressional pulse in a crystal of the order of 1 cm in diameter is dispersive, and the pulse shape changes as it propagates through the crystal. The reflected pulse indicates an appreciable acoustic mismatch in the bar assembly.

6. Torsion Stress Pulses

Pope, et. al. have described a machine for producing single, square, torsion pulses of microsecond duration.[19] This machine

generates a zero mode torsional wave front with a rise time of 2 μsec in a 1/2 in. cylindrical, elastic rod. Zero mode torsional waves in elastically isotropic rods are non-dispersive. They are also non-dispersive in cylindrical rods of HCP crystals with an [0001] axis, and in cubic crystals with a [100] axis. The wave front is generated by the sudden release of a torsional constraint on a twisted cylindrical rod. The wave front propagates from an isotropic elastic rod into a specimen crystal. The material of the elastic rod is chosen such that its acoustic impedance for shear waves is nearly equal to that of the test crystal. Compensation for small differences in the acoustic impedances can be made by choosing the rod diameters such that

$$\left(m_o c J\right)_{\text{rod 1}} = \left(m_o c J\right)_{\text{rod 2}} \tag{8}$$

where J = polar moment of inertia of the cross section. Torsional wave fronts with a 2 μsec rise time have been made to pass through interfaces between cylindrical rods of titanium and aluminum, titanium and monel, steel and copper, and steel and quartz without a measurable reflection, when the rod diameters are adjusted such that Eq. 8 is satisfied. The loading wave front, after passing through the specimen crystal, is reflected at a free surface normal to the cylindrical axis. The reflected wave unloads the specimen, and the duration of loading at any point in the crystal is just the round trip travel time of the wave front from that point to the free end. The rod system is constructed such that all wave fronts traveling away from the specimen are dispersed, and the majority of their energy is dissipated so that they do not subsequently reflect and produce appreciable stresses in the

specimen. The torsion strain on the surface of the elastic rod is monitored using semiconductor strain gages. A strain vs. time record of the passage of the loading and unloading wave fronts is shown in Fig. 3. Examples of the use of torsion stress pulse in dislocation velocity measurements are given in section IV.

7. Stress Pulses Produced by Detonation Waves

Carlsson and Gilman employed simultaneous explosions of lead azide at the two ends of a crystal bar to obtain short duration stress pulses.[20] The elastic pulses generated by the explosions meet and reinforce at the center of the bar to produce transient plastic flow, and the pulse length is sufficiently short to allow near-sonic dislocation velocities to be measured. Ignition at the two ends was achieved by the simultaneous exploding of tungsten wires which were in contact with the explosives and electrically connected in parallel. A capacitor, discharged through the tungsten wires, provided the energy to ignite the explosive. The stress magnitude was varied by varying the specimen cross section and the amount of explosive used. A strain vs. time record of the main pulse and a more distorted, reflected pulse is shown in Fig. 4a. The finite length of the strain gage would make even a square pulse appear as shown in Fig. 4b. Thin bars must be used in this experiment since the minimum pulse length is limited by dispersion of the wave. The effect of the reflected pulses which are trapped in the specimen can be ignored if they produce dislocation velocities which are negligible compared to that produced by the reinforced, main pulses.

IV. Direct Measurements of Dislocation Velocity

A. The Ionic Crystals, LiF and NaCl

Johnston and Gilman made the first measurements of velocities of individual dislocations in crystals covering a range of twelve orders of magnitude in velocity.[21] Velocities between 5×10^{-7} and 10^{-3} cm/sec were produced in 2 x 6 x 35 mm specimens of LiF loaded by dead weights in a four point bending fixture. Velocities between 10^{-3} and 10 cm/sec were produced by use of the four point bending fixture loaded by the magnetic pulsing machine shown in Fig. 1a. Velocities between 10 and 5×10^{4} cm/sec were produced by the use of the impact system shown in Fig. 2a. Specimens were cleaved to the desired size, and chemically polished to remove dislocations produced by the cleavage. Small $\{110\}\langle 1\bar{1}0\rangle$ half loops were produced at the surface as depicted in Fig. 5. A specimen containing fresh loops was etched and subjected to a stress pulse. The crystal was etched again and the individual dislocation movements were measured. At least 40 measurements were made to determine one average velocity point. A considerable scatter was observed in the measurements, the standard deviation being about 30% of the average of the measurements. No dislocation movement as great as 1μ was observed at 600 g/mm^2 in 10^5 sec; at 650 g/mm^2 only about 2 or 3% of the fresh dislocations moved; at 700 g/mm^2 about 20% moved; and above 800 g/mm^2 all fresh dislocations moved during each test. The stress dependence of the average dislocation velocity is shown in Fig. 6. At low velocities, the data follows the relation

$$v = (\underline{\tau}/\underline{\tau}_o)^n \qquad (9)$$

where τ_o is the stress required to produce unit velocity and n is called the mobility exponent. The velocity of the edge oriented dislocations is about 50 times greater than that of the screw oriented dislocations at the lower velocities (the mobility exponent is nearly the same, n = 25, but τ_o is smaller for edge than for screw dislocations). The curves converge as they approach the shear wave velocity. The dislocation displacement produced by 10 pulses of 40 msec was essentially the same as the displacement produced by a single 400 msec pulse of the same stress magnitude (1 kg/mm^2). The dislocation velocity at a fixed stress was found to vary exponentially with 1/T (+25°C > T > -50°C), and the effects of impurities, heat treatment, and neutron radiations were examined.

Gutamas, Nadhornyi, and Stepanov[22] measured dislocation velocities in NaCl using techniques similar to those of Johnston and Gilman. A comparison of their results for screw oriented dislocations in NaCl of two different purities with those for LiF is shown in Fig. 7, where the log of dislocation velocity is plotted against the reciprocal of stress. At high velocities the data obeys the relation

$$v = v^* \exp(-D/\tau) \qquad (10)$$

where v* is the limiting velocity, and D is a constant. The limiting velocity appears to be near the shear wave velocity. The data for high purity NaCl deviate from Eq. 10 at low stresses where higher velocities are observed. Short-range dislocation-impurity interactions are thought to limit the dislocation mobility in the LiF and NaCl crystals.[23] Gilman has shown that such interactions can lead to the stress dependence given

by Eq. 10, and has suggested that impurity drift is responsible for the deviation from Eq. 10 observed at low velocities in NaCl.[23]

B. The Semiconductor Crystals

Chaudhuri, Patel, and Rubin[24] measured average dislocation velocities in four semiconductor crystals--silicon, germanium, gallium antimonide, and indium antimonide. Both the temperature and stress dependence of dislocation velocity were measured. Specimen crystals 4.5 cm long x 0.3 cm wide x 0.2 cm were prepared which were initially free of dislocations with the wider face either (100) or (111). A scratch was made along the length of the wide face with a sapphire stylus, and the crystal was etched to remove some of the scratch damage. The specimens were manually loaded in three point bending. Upon re-etching it was observed that slip bands had moved out from the scratch. Velocity measurements were also made on specimens loaded in compression. The motion of dislocation loops formed by the scratch was not linear with time in the region very close to the scratch. After moving a distance comparable to the scratch width the motion was linear with time. Dislocation motion was greatest at the loading point and diminished to zero at the specimen supports. No orientation dependence of dislocation velocity was found, and it was concluded that in all instances mixed 60° dislocations were observed. Measurements were made over about one order of magnitude in velocity at each temperature, in the velocity range of 10^{-6} to 2×10^{-1} cm/sec. The stress dependence of dislocation velocity, as expressed by Eq. 9, for the four materials tested at various temperatures is given in Table I. The velocities in the semiconductor crystals

are relatively insensitive to stress compared to the velocities in LiF and NaCl.

TABLE I

Stress Dependence of Dislocation Velocities in Semiconductor Crystals (after Chaudhuri, et. al.[24])

	Temperature °C	n	τ_o (kg/mm^2)
Germanium	420	1.51	2480
	440	1.65	844
	476	1.32	1900
	500	1.90	158
	525	1.66	206
	550	1.65	145
	575	1.35	195
	600	1.46	85
	700	1.51	17
Silicon	600	1.4	3500
	753	1.5	600
	800	1.4	440
	940	1.4	112
Gallium antimonide	450	2.0	39
Indium antimonide	218	1.87	42

The temperature dependence of dislocation velocity in germanium was found to fit the expression

$$v = v_o(\underline{\tau}) \exp(-E/kT) \qquad (11)$$

where $v_o(\underline{\tau})$ is a function of stress, and the activation energy E is essentially independent of stress. An activation energy between that of the formation and motion of a vacancy was found.

Motion of dislocations from a scratch in germanium was observed by D. Dew-Hughes.[25] Specimens with [321] and [110] axes were pulse loaded in tension, and higher velocities were observed at the same stress level

in crystals that had been zone-leveled rather than tested as-pulled. This was attributed to a higher vacancy concentration in the as-pulled crystals.

The velocities of individual half-loops in germanium crystals was studied by Kabler.[26] Fresh half-loops were introduced by scratching and applying stress for a short time at around 730°K. The scratch and most of the half-loops were then polished off, leaving a smooth surface containing a suitable number of isolated dislocations. The diameters of the half-loops were always small compared to the 0.9 x 1.5 x 33 mm specimen dimensions. Etching in depth and etching on exposed (111) slip planes showed the half loops to be half-hexagons. Specimens were oriented such that the largest surfaces were (111) and the axis was $[\bar{1}01]$. The specimens were heated to the test temperature by passing a direct current through the crystals while they were in a three point bending fixture (test temperatures were in the intrinsic conductivity range). Dead Weight loading was applied to the bending fixture for periods ranging from 1 sec to 10 h. Typical shapes and movements of the half-hexagons on $(11\bar{1})$ slip planes observed by Kabler are illustrated in Fig. 8. The 60° segments glide further at high stresses (10 kg/mm^2) than do the screw oriented segments, while the reverse is true at low stresses (0.5 kg/mm^2). A velocity point was obtained by averaging 40 to 100 individual displacement measurements and dividing by the duration of loading (the actual dislocation velocity, normal to the dislocation line, is $\sqrt{3}/2$ of the reported velocity). It was observed that groups of dislocations gliding together as a slip band moved up to several times as fast as isolated dislocations of the same orientation, and this effect

diminished at high stress. In view of this, reasonable agreement was found with the results of Chaudhuri, et. al.[24] for dislocation velocities in germanium in the same range of temperature and stress.

Suzuki and Kojima[27] employed the Lang X-ray technique to determine dislocation positions in thin crystals of silicon. Screw dislocation velocity was determined at 600°, 700°, and 800°C as a function of resolved shear stress up to about 40 kg/mm^2. Crystals in the form of small beams, 0.7 x 2.7 x 20 mm, were oriented with the $[11\bar{2}]$ normal to the side surfaces and the $[1\bar{1}0]$ slip direction was in the side surface and at 45° to the long edges. The specimens were loaded in 3-point bending such that the stress rate at any point in the specimen was approximately constant. When a predetermined maximum stress was reached, the specimens were rapidly unloaded, and an X-ray photograph taken. The loading procedure was repeated at successively higher loads up to the macroscopic yield point of the crystal. Dislocation displacements were obtained after each loading by measuring the growth of fresh dislocation loops which generated at undetermined sources within the crystals (presumably impurity aggregates which produced no observable image in the X-ray photographs). The dislocation velocity at each value of maximum stress was calculated using the maximum stress, stress rate, and displacement values from that loading, and the values of stress and dislocation velocity obtained at the lower stress levels of the preceding loadings. While this procedure permits the use of a triangular load pulse rather than a square pulse, the cumulative nature of the calculations requires very good accuracy in the determination of stress, stress rate, and dislocation displacement to keep the uncertainty in dislocation velocity small. Values of τ_o

determined from these experiments agree well with the results of Chaudhuri, et. al.[24] for 60° dislocations while the values of n were somewhat higher, (1.85 vs. 1.4 at 800°C).

The observation that glide dislocations in the semiconductor crystals have a strong preference to lie straight along crystallographic directions indicates that the Peierls energy is high in these crystals. Theoretical treatments of dislocation glide over the Peierls barrier by the nucleation and motion of kinks have been made and compared to the observed stress and temperature dependence of dislocation mobility in germanium[23,28] and in silicon[27]. It is interesting to note that the limiting dislocation velocity is not the velocity of shear waves in this case. The limiting velocity of kinks should be equal to the shear wave velocity. The net dislocation velocity depends upon the concentration of kinks and is much less than the kink velocity for all but exceedingly high concentrations of kinks.

C. The Body Centered Cubic Metals, Fe and W

Stein and Low[29] measured the mobility of edge dislocations in 3 1/4% silicon-iron crystals on {110} slip planes over a velocity range of 10^{-7} to 10^{-2} cm/sec. Their method utilized an etching technique to reveal the distance which dislocations moved from a scratch as a result of pulse loading. The etching reveals dislocation-surface intersections when carbon is segregated to the dislocations. Aging of lightly deformed

specimens for 15 min at 160°C was sufficient to segregate sufficient carbon to fresh dislocation sites. The aging treatment does not cause significant changes in the positions of the dislocations. Specimens 30 mm x 2.5 mm x 0.8 mm were oriented as shown in Fig. 9. The crystals were scratched on a (112) surface at 78°K and held at that temperature until ready for loading to prevent migration of impurities to the fresh dislocations. Specimens were loaded in a three point bending fixture for times ranging from 2 sec to 2 h. The dislocation motion was much more rapid within about 8μ of the scratch (one scratch width) than beyond that distance. Dislocation displacements large compared to 8μ were measured. Velocities were computed by dividing the measured displacement, less a correction factor of 8μ, by the pulse duration. The mobility data at four temperatures is given in Table II. The large mobility exponent indicates a relatively large stress dependence for dislocation velocity in silicon-iron.

Erickson[31] measured the mobility of edge dislocations on {112} slip planes of silicon-iron. The crystal orientation shown in Fig. 10 was used, and four point bending produced a 15% larger resolved shear stress on a (112) than on any {110} plane in the crystal. The crystals were scratched using essentially the same technique as that of Stein and Low except that the direction of scribing was found to be important. Scribing in the direction shown in Fig. 10 produced a larger number of mobile dislocations than did scribing in the opposite direction. Erickson's values of n and τ_o for edge dislocations on the {112}⟨111⟩ slip system at three temperatures in silicon iron are given in Table II.

TABLE II

Values of n and τ_o for edge dislocations on {110} and {112} planes in Silicon Iron after Stein and Low[29] and Erickson[30]

	n		τ_o(10^9 dynes/cm^2)	
T°K	{110}[29]	{112}[30]	{110}[29]	{112}[30]
78	44		3.8	
198	38	42	2.3	2.48
233		43		2.20
298	35	34	2.0	1.93
373	41		1.5	

Moon[31] has measured dislocation velocities in single crystals and in individual grains of polycrystalline silicon iron using tensile load pulses and the scratching and etching technique of Stein and Low. Small variations of stress across a grain, due to crystal anisotropy and the difference in orientation of neighboring grains, may produce a large variation in dislocation velocity in the grain due to the large mobility exponent. Slip bands in a polycrystalline specimen which moved away from a scratch during a tensile stress pulse are shown in Fig. 11. The variation in dislocation displacement across most of the grains was found to be small. The orientation of the grains in which dislocation displacements could be observed was determined (by use of a Unitron microgoniometer) and the nominal resolved shear stress calculated by means of Eq. 7. Low and Guard[32] have shown that dislocation loops in silicon iron are very much elongated in the direction of the Burgers vector. This indicates an appreciably larger velocity for edge oriented dislocations than for screw oriented dislocations at the same stress. The slip bands seen on the surface in the polycrystalline grains tested by Moon must be considerably elongated in the direction of the Burgers vector. We therefore expect that the rate of growth of all of the slip bands measured was essentially equal

to the velocity of the screw components, since none of the grains in which measurements were made had a Burgers vector which intersected the slip trace at a small angle. This is also true of the single crystal velocity measurements shown in Fig. 12. The velocity of edge dislocations measured by Stein and Low is indicated by the dashed line in Fig. 12. Average dislocation velocity on {110} planes vs. nominal resolved shear stress in a number of grains is shown in Fig. 12. The scatter is considerably greater than that found in single crystals, and is presumably due to differences between the nominal and actual resolved shear stress. The screw dislocation velocity in single crystals is considerably less than the edge dislocation velocity at the same stress. The data for polycrystalline specimens can be considerably biased by the selection of the pulse duration at a particular stress level. Significant measurements can be made only in those grains in which the dislocations do not reach the grain boundaries but move distances at least comparable to the scratch width. A relatively long duration pulse will cause loss of data from grains in which the resolved stress is high since the dislocations in these grains will reach the grain boundaries. A relatively short duration pulse will produce data in only those grains which have a high resolved stress since these will be the only grains in which the displacements are large enough to measure. A relatively short pulse duration was chosen for the tests on polycrystalline silicon-iron specimens to obtain data from the more highly stressed grains. The data from these grains therefore lie above the curve for the single crystal specimens, and is closer to the curve for edge oriented dislocations in silicon-iron.

It would be of considerable interest to determine the effect of carbon on the dislocation mobility in silicon-iron. Since the etching technique for this material depends upon the presence of a relatively critical amount of carbon, another technique for dislocation observation must be used in such a study.

Schadler[33] measured edge dislocation velocities on the {110}⟨111⟩ slip system of tungsten by a technique similar to that employed by Stein and Low. Crystals oriented as in Fig. 9 were scratched and subjected to three point bending, and average dislocation velocities from approximately 10^{-5} to 10^{-1} cm/sec were measured. Average values of n and $\log_{10} \tau_o$ at two temperatures are given in Table III.

TABLE III

Values of n and $\log_{10} \tau_o$ for edge dislocations in the {110}⟨111⟩ slip system of tungsten after Schadler.[33]

T°K	n	$\log_{10} \tau_o$ (psi)
77	10.5	4.79
298	4.8	4.65

D. The HCP and FCC Metals, Zn and Cu

Measurement of dislocation velocities in soft metal crystals is complicated by the difficulties of obtaining and maintaining a low density of mobile dislocations in the crystals. The stress dependence of dislocation velocity is difficult to measure in some soft crystals because the velocity of the dislocations changes from zero to a relatively high value at a low resolved shear stress. Adams[34] has observed such a discontinuous behavior of dislocation velocity with stress in the (0001)⟨$\bar{1}2\bar{1}0$⟩ basal

slip system of zinc. One half in. cube specimens of the orientation shown in Fig. 13a were etched to reveal the dislocation structure on the two $(10\bar{1}0)$ surfaces, pulse loaded, and re-etched. No motion was observed below a resolved shear stress of 6 psi, but at stresses in excess of 6 psi slip bands form very rapidly. The average dislocation velocity at the break-away stress is approximately 7 cm/sec. Stresses above 12 psi applied for 17 msec drive slip bands entirely across the specimen, indicating an average velocity (of the leading dislocations) in excess of 70 cm/sec. The velocity of edge dislocations in slip bands on the $\{1\bar{2}12\}$ $\langle 1\bar{2}1\bar{3}\rangle$ second order pyramidal slip system in zinc was also measured using the pulse loading and etching technique. Basal slip was minimized in these tests by orienting the compression specimens as shown in Fig. 13b. The $(10\bar{1}0)$ surfaces can be etched to reveal dislocations. Edge oriented dislocation velocities between 10^{-4} and 2 cm/sec at 300°K obey Eq. 9 with $n = 9.5$ and $\tau_o = 790$ psi. Blish[35] is currently measuring the mobility of both edge and screw segments on the $\{1\bar{2}12\}$ $\langle 1\bar{2}1\bar{3}\rangle$ slip system of zinc using compression specimens oriented as shown in Fig. 13c. The compression axis is $[1\bar{2}10]$, and the basal system has no resolved shear stress. Two second order pyramidal planes, $(1\bar{2}12)$ and $(\bar{1}2\bar{1}2)$ are stressed, while the $(10\bar{1}0)$ surfaces and $(\bar{1}01\ 24)$ surfaces (the latter a plane 5° from the basal plane) are etched. The $(\bar{1}01\ 24)$ is not normal to $(10\bar{1}0)$ so the cross section of the crystal is a parallelogram. Edge dislocation intersections are seen on the $(10\bar{1}0)$ surfaces while the dislocations intersecting $(\bar{1}01\ 24)$ are close to pure screw orientation (it is assumed that the dislocations make a near-normal intersection with the trace of the slip plane at the surface).

slip system of zinc. One half in. cube specimens of the orientation shown in Fig. 13a were etched to reveal the dislocation structure on the two $(10\bar{1}0)$ surfaces, pulse loaded, and re-etched. No motion was observed below a resolved shear stress of 6 psi, but at stresses in excess of 6 psi slip bands form very rapidly. The average dislocation velocity at the break-away stress is approximately 7 cm/sec. Stresses above 12 psi applied for 17 msec drive slip bands entirely across the specimen, indicating an average velocity (of the leading dislocations) in excess of 70 cm/sec. The velocity of edge dislocations in slip bands on the $\{1\bar{2}12\}\langle 1\bar{2}1\bar{3}\rangle$ second order pyramidal slip system in zinc was also measured using the pulse loading and etching technique. Basal slip was minimized in these tests by orienting the compression specimens as shown in Fig. 13b. The $(10\bar{1}0)$ surfaces can be etched to reveal dislocations. Edge oriented dislocation velocities between 10^{-4} and 2 cm/sec at 300°K obey Eq. 9 with $n = 9.5$ and $\underline{\tau}_o = 790$ psi. Blish[35] is currently measuring the mobility of both edge and screw segments on the $\{1\bar{2}12\}\langle 1\bar{2}1\bar{3}\rangle$ slip system of zinc using compression specimens oriented as shown in Fig. 13c. The compression axis is $[1\bar{2}10]$, and the basal system has no resolved shear stress. Two second order pyramidal planes, $(1\bar{2}12)$ and $(\bar{1}2\bar{1}2)$ are stressed, while the $(10\bar{1}0)$ surfaces and $(\bar{1}01\ 24)$ surfaces (the latter a plane 5° from the basal plane) are etched. The $(\bar{1}01\ 24)$ is not normal to $(10\bar{1}0)$ so the cross section of the crystal is a parallelogram. Edge dislocation intersections are seen on the $(10\bar{1}0)$ surfaces while the dislocations intersecting $(\bar{1}01\ 24)$ are close to pure screw orientation (it is assumed that the dislocations make a near-normal intersection with the trace of the slip plane at the surface).

Slip bands which formed in a short duration pulse on both $(10\bar{1}0)$ and $(\bar{1}01\ 24)$ surfaces are shown in Fig. 14. Many of the slip bands start from the sub-boundaries. The length of the slip bands on both surfaces is about the same, so edge and screw components travel at about the same velocity. Attempts to produce mobile, fresh dislocations on $(10\bar{1}0)$ surfaces of zinc by various kinds of surface damage have not been successful, and in each test the mobile dislocations originate at the sub-boundaries or at other grown-in defects, rather than at the surface damage.

Pope[36] has applied the Berg-Barrett technique to reveal basal dislocations which lie within several microns of a (0001) basal surface in zinc. Crystals in the form of [0001] axis cylinders are prepared by acid machining with a relatively low dislocation density. The crystals contain a substructure which consists primarily of tilt boundaries, and the Berg-Barrett plates show a very low density of basal dislocations within the sub-grains, less than 1 cm of dislocation per cm^2 of plate (due in part to the small penetration depth of the X-rays). The (0001) surface of a crystal was intentionally damaged by thermal shock (touching it with a hot teflon rod wet with oil) and a Berg-Barrett photograph of the $(10\bar{1}3)$ reflection from the surface was made. Several sub-boundaries and basal dislocations resulting from the thermal shock may be seen on the enlarged print, Fig. 15a. The (0001) surface of the crystal was then subjected to a torsion pulse generated by the system described in section III. The torsion stress wave passes from a monel rod, through a glue bond into the crystal (monel is used to match the thermal coefficient of expansion in the basal plane of the crystal). The glue bond is then removed with a

suitable solvent, and a second Berg-Barrett photograph taken of the (0001) surface. Dislocation motion away from the thermal damage was noted, and the substructure was observed to break-up, emitting a large number of dislocations, Fig. 15b. Break-up of a sub-boundary has also been observed by etching of the cylindrical surface of a specimen which was subjected to a torsional stress pulse, Fig. 16 (etching reveals dislocation intersections on surfaces ±5° to the $\{10\bar{1}0\}$, so six areas around the cylindrical surface are etched).

Quantitative measurements of dislocation mobility in copper are being made by Greenman[37] using the torsion pulse technique. Dislocations on the {100} surfaces are revealed by etching. Cylinders of approximately 1/2 in. diameter with a [100] axis, and four {100} flats approximately 2-3 mm wide, are cemented to a polycrystalline copper cylinder which in turn is cemented to a steel rod of the torsion pulsing machine (the polycrystalline copper is provided to minimize thermal stressing of the single crystal test specimen). The specimen is scratched prior to the stress pulse test, etched after scratching, and etched again immediately after stressing. Plastic replicas of the etched surfaces are made, and compared using a "blink" microscope[38] especially designed for the critical comparison of replicas (or X-ray photographs). Dislocation displacements are measured using a filar eyepiece in the microscope. Naked edge-screw dislocations are subjected to the maximum resolved shear stress (assuming that the dislocations make a near-normal intersection with the slip trace on the surface. Photomicrographs of a scratched and etched surface, before and after application of a stress pulse are shown in Fig. 17. The results of a number of displacement measurements on a copper crystal are shown in Fig. 18. The average displacement is

plotted, the bars showing the standard deviation and the numerals indicating the number of individual measurements represented by each point. The abscissa of Fig. 18 may be converted to a "time at stress" axis using the known shear wave velocity (the pulse duration at any point in the specimen is just the time for the stress wave to travel from that point to the free end, and return). The linearity of the dislocation displacement vs. time at stress is apparent. The velocity data for copper at room temperature shows the mobility exponent to be relatively low (on the order of one), and velocities to be relatively high at low stresses (10^3 cm/sec at about 150 gm/mm^2).

V. Indirect vs. Direct Measurements of Dislocation Velocity

A number of investigators have attempted to deduce the stress dependence of dislocation velocity from macroscopic measurements alone. Two commonly employed techniques involve determination of the strain rate sensitivity of the flow stress,[39] and determination of the rate of stress-relaxation at constant total strain.[40] Interpretation of these experiments to deduce the stress dependence of the dislocation velocity requires a knowledge of the stress dependence of the moving dislocation density ρ_m, since the plastic strain rate is proportional to the product of the two "microscopic" variables, ρ_m and $\bar{v}$.

The indirect methods of deducing the mobility exponent in Eq. 9 have been applied to the following materials in which direct mobility measurements have been made: iron-3.25% silicon single crystals and polycrystals, and single crystals of LiF, tungsten, zinc, and copper. Johnston and Stein[41] find agreement between n obtained by direct measurement of the stress-velocity relationship and the mobility exponent inferred from the strain rate sensitivity at low strains in silicon-iron and LiF, when the stress dependence of ρ_m is ignored. Guard[39] and Noble and Hull[40] found that the indirectly determined n in silicon-iron, assuming ρ_m = constant, was larger than the n determined by Stein and Low,[29] even at low values of strain. Schadler[33] found a similar result for tungsten and concluded that the stress dependence of ρ_m cannot be ignored. Adams[34] found that the stress dependence of ρ_m was more important than the stress dependence of dislocation velocity in Zn. The directly determined mobility exponent in high purity copper crystals is of the order of unity,[37] while values between

100 and 200 have been found in indirect measurements[42] (when the stress dependence of ρ_m is ignored).

It is apparent that the stress dependence of ρ_m cannot be ignored in crystals with a relatively high density of mobile dislocations. This condition is found at very low strains in the soft crystals such as Zn and Cu, and at higher strains in relatively harder LiF and silicon iron. Bell and Bonfield[43] inferred a mobility exponent of approximately 7 from the strain rate sensitivity of Ge in the ideal eazy glide region where the total dislocation density remains constant. A comparison of this mobility exponent with the mobility exponent of approximately 1.5 observed in the direct measurements of Chaudhuri et. al.[24] in Ge indicates that the stress dependence of ρ_m may be important even under conditions where the total dislocation density ρ_t is constant.

The differences between the direct and indirect observations of the stress dependence of dislocation velocity may also be attributed to the effect of dislocation interactions. Relatively low dislocation densities are the rule in the direct observations while the indirect observations are made at total strain levels which are generally large compared to the elastic strains, so that ρ_t is larger in the indirect tests. Additional experimental work involving measurements of both the macroscopic parameters of strain, stress, and time, and the microscopic parameters ρ_m, ρ_t, and v is needed before these questions of the stress dependence of dislocation velocity can be resolved.

REFERENCES

1) J. J. Gilman, "Progress in the Microdynamical Theory of Plasticity," Proceedings 5th U. S. Nat. Congr. Appl. Mech., Amer. Soc. Mech. Engrs.

2) W. G. Johnston, "Yield Points and Delay Times in Single Crystals," J. Appl. Phys. 33, 2716 (1962).

3) J. C. M. Li, "A Dislocation Mechanism of Transient Creep," Acta Met. 11, 1269 (1963).

4) J. W. Taylor, "Dislocation Dynamics and Dynamic Yielding," J. Appl. Phys. 36, 3146 (1965).

5) F. C. Frank, "On the Equations of Motion of Crystal Dislocations," Proc. Phys. Soc. A 62, 131 (1949).

6) R. Thomson, Discussion of Paper "High Velocity Dislocations" by J. Weertman, Response of Metals to High Velocity Deformation (Interscience Publishers, New York, 1961), p. 246.

7) J. D. Eshelby, "Uniformly Moving Dislocations," Proc. Phys. Soc. A 62, 307 (1949).

8) J. F. Butler, "Lüders Front Propagation in Low Carbon Steels," J. Mech. Phys. Sol. 10, 313 (1962).

9) R. Siems and P. Haasen, "The Velocity of Twinning in Zinc Single Crystals," Z. Metallkunde 49, 213 (1958).

10) D. W. Bainbridge, C. H. Li, and E. H. Edwards, "Recent Observations on the Motion of Small-Angle Dislocation Boundaries," Acta Met. 2, 322 (1954).

11) T. Vreeland, Jr., "Tilt Boundary Motion in Zinc Produced by Static and Dynamic Shear Stress," Acta Met. 9, 112 (1961).

12) E. S. Machlin, "Thermal Etching of Dislocations in Silver," Dislocations and Mechanical Properties of Crystals, (John Wiley & Sons, 1957), p. 164.

13) J. J. Gilman and W. G. Johnston, "The Origin and Growth of Glide Bands in Lithium Fluoride Crystals," Dislocations and Mechanical Properties of Crystals, (John Wiley & Sons, 1957), p. 116.

14) H. S. Chen, J. J. Gilman, and A. K. Head, "Dislocation Multipoles and Their Role in Strain Hardening," J. Appl. Phys. 35, 2502 (1964).

15) R. F. S. Hearmon, Applied Anisotropic Elasticity (Oxford University Press, 1961), p. 52.

16) W. G. Johnston and J. J. Gilman, "Dislocation Velocities, Dislocation Densities, and Plastic Flow in Lithium Fluoride Crystals," J. Appl. Phys. 30, 129 (1959).

17) D. S. Clark and D. S. Wood, "The Time Delay for the Initiation of Plastic Deformation at Rapidly Applied Constant Stress," Proc. Am. Soc. Testing Mats. 49, 717 (1949).

18) H. Kolsky, Stress Waves in Solids (Oxford University Press, 1953), p. 44.

19) D. P. Pope, T. Vreeland, Jr. and D. S. Wood, "Machine for Producing Square Torsion Pulses of Microsecond Duration," Rev. Sci. Instr. 35, 1351 (1964).

20) A. J. Carlsson and J. J. Gilman, "Method for Measuring Sonic Dislocation Velocities," Rev. Sci. Instr. 34, 860 (1963).

21) E. V. Gutmanas, E, M, Nadgornyi, and A. V. Stepanov, "Dislocation Movement in Sodium Chloride Crystals," Soviet Phys. - Solid State 5, 743 (1963).

22) R. L. Fleischer, "Rapid Solution Hardening, Dislocation Mobility, and the Flow Stress of Crystals," J. Appl. Phys. 33, 3504 (1962).

23) J. J. Gilman, "Dislocation Mobility in Crystals," J. Appl. Phys. 36, 3195 (1965).

24) A. R. Chaudhuri, J. R. Patel, and L. G. Rubin, "Velocities and Densities of Dislocations in Germanium and Other Semiconductor Crystals," J. Appl. Phys. 33, 2736 (1962).

25) D. Dew-Hughes, "Dislocations and Plastic Flow in Germanium," IBM J. Res. Develop. 5, 279 (1961).

26) M. N. Kabler, "Dislocation Mobility in Germanium," Phys. Rev. 131, 54 (1963).

27) T. Suzuki and H. Kojima, "Dislocation Motion in Silicon Crystals as Measured by the Lang X-Ray Technique," Accepted for publication in Acta Met, 1966.

28) V. Celli, M. Kabler, T. Ninomiya, and R. Thompson, "Theory of Dislocation Mobility in Semiconductors," Phys. Rev. 131, 58 (1963).

29) D. F. Stein and J. R. Low, Jr., "Mobility of Edge Dislocations in Silicon-Iron Crystals," J. Appl. Phys. 31, 362 (1960).

30) J. S. Erickson, "Mobility of Edge Dislocations on {112} Slip Planes in 3.25% Silicon Iron," J. Appl. Phys. 33, 2499 (1962).

31) D. W. Moon, Research in Progress, W. M. Keck Laboratory of Engineering Materials, Calif. Inst. of Technology, Pasadena.

32) J. R. Low, Jr. and R. W. Guard, "The Dislocation Structure of Slip Bands in Iron," Acta Met. 7, 171 (1959).

33) H. W. Schadler, "Mobility of Edge Dislocations on {110} planes in Tungsten Single Crystals," Acta Met. 12, 861 (1964).

34) K. H. Adams, "Dislocation Mobility and Density in Zinc Single Crystals," Thesis, California Institute of Technology, University Microfilms No. 65-11,064.

35) R. C. Blish, Research in Progress, W. M. Keck Laboratory of Engineering Materials, California Institute of Technology, Pasadena.

36) D. P. Pope, Research in Progress, W. M. Keck Laboratory of Engineering Materials, California Institute of Technology, Pasadena.

37) W. F. Greenman, Research in Progress, W. M. Keck Laboratory of Engineering Materials, California Institute of Technology, Pasadena.

38) D. P. Pope, T. Vreeland, Jr., and D. S. Wood, "Comparison System for Microscipe Images," Rev. Sci. Instr. 37. 377 (1966).

39) R. W. Guard, "Rate sensitivity and dislocation velocity in silicon iron," Acta Met. 9, 163 (1961).

40) F. W. Noble and D. Hull, "Stress dependence of dislocation velocity from stress relaxation experiments," Acta Met. 12, 1089 (1964).

41) W. G. Johnston and D. F. Stein, "Stress dependence of dislocation velocity inferred from strain rate sensitivity," Acta Met. 11, 317 (1963).

42) H. Conrad, "An Investigation of the Rate Controlling Mechanism for Plastic Flow of Copper Crystals at 90° and 270°K," Acta Met. 6, 339 (1958).

43) R. L. Bell and W. Bonfield, "The Plastic Deformation of Germanium Single Crystals: Yield and Ideal Easy Glide," Phil. Mag. 9 9 (1964).

FIGURE CAPTIONS

1. (a) Magnetic pulsing machine with a pulsed coil in a magnetic gap loading a four point bending fixture (after Johnston and Gilman[16]).

   (b) Stress pulse shape obtained from the magnetic pulsing machine.

2. (a) Impact system in which a CO_2 gun fires a 1/16 in. diameter ball-bearing through baffle plates to strike a bar assembly which is supported as a ballistic pendulum (after Johnston and Gilman[16]).

   (b) The main stress pulse and a smaller reflected pulse indicated by the barium titanate transducer in the bar assembly.

3. A torsion stress pulse of 1000 psi indicated by silicon piezoresistance strain gages located 6.4 in. from the free end of a 1/2 in. diameter titanium rod (0.050 in. gage length mounted at 45° to rod axis). The upper trace indicates that only a single stress pulse is obtained, and the lower trace shows the pulse shape on an expanded time scale (after Pope, et. al.[19]).

4. (a) Stress pulses in a steel specimen produced by detonation waves as measured by a strain gage 0.3 cm long mounted axially (after Carlsson and Gilman[20]).

   (b) Expected output for a square stress pulse of 0.5 cm length showing the effect of the 0.3 cm strain gage length.

5. Schematic drawing of two dislocation loops that intersect the surface of a cleaved crystal of LiF, screw components emerge at points S and edge components emerge at points E (after Johnston and Gilman[16]).

6. Log-log plot of dislocation velocity vs. resolved shear stress in an as-grown LiF crystal (after Johnston and Gilman[16]).

7. Log of screw dislocation velocity vs. the reciprocal of the resolved shear stress in NaCl of two different purities, NaCl-I contained 10^{-3}% Ca and NaCl-III contained on the order of 10^{-2}% Ca (after Gutmanas et. al.[21]). The dashed line represents the behavior of screw dislocations in LiF from the data of Fig. 6.

8. Typical shapes and movements of half-loops in Germanium (after Kabler[26]). The behavior of dislocations with the two possible Burgers vectors, at high and low applied stress, is indicated.

9. Orientation of the silicon-iron crystals used by Stein and Low[29] to study the mobility of edge oriented dislocations on the {110}<111> system. The crystals were scratched on the top (112) face, and bent about an axis which lies in a (112) plane and is normal to the long edge.

10. Orientation of the silicon-iron crystals used by Erickson[30] to study the mobility of edge dislocations on the {112}<111> system. The crystals were scratched on the top (110) face in the direction indicated, and bent about an axis which lies in a (110) plane and is normal to the long edge.

11. Slip band growth in a polycrystalline silicon-iron specimen scratched with a diamond stylus (after Moon[31]). Tensile stress pulse, 4.09×10^9 dyne/cm^2, 17 msec duration.

12. Screw dislocation velocity vs. resolved shear stress on {110}<111> in single and polycrystalline silicon-iron specimens at room temperature (after Moon[31]). The dashed line is for edge dislocations in single crystals (after Stein and Low[29]).

13. Orientation of compression specimens of zinc.[33,34] Load is applied to the top and bottom surfaces of the crystals. (a) Oriented for basal (0001)$\langle\bar{1}2\bar{1}0\rangle$ slip. (b) Oriented for simultaneous slip on the six $\{1\bar{2}12\}\langle 1\bar{2}13\rangle$ second order pyramidal slip systems. (c) Oriented for slip on two planes of the $\{1\bar{2}12\}\langle 1\bar{2}13\rangle$ system.

14. Slip bands on the $\{1\bar{2}12\}\langle 1\bar{2}13\rangle$ system of zinc which formed during a stress pulse, 425 psi, 17 msec duration, $[1\bar{2}10]$ compression axis is vertical. (a) $(10\bar{1}0)$ surface, edge components. (b) $(\bar{1}01\ 24)$ surface, screw components.

15. Berg-Barrett photographs of the $(10\bar{1}3)$ reflection from a (0001) surface of zinc, Cobalt Kα radiation. (a) Sub-boundaries and thermal shock damage. (b) Same area after a torsional stress pulse was applied to the (0001) surface.

16. Substructure break-up produced by a torsional stress pulse revealed on an etched $(10\bar{1}0)$ surface of zinc. (a) Before stress pulse test. (b) Re-etched after the application of a stress pulse.

17. A scratched and etched (010) surface of a copper crystal 13.5 mm from the free end. (a) Before stress pulse test. (b) Re-etched after the application of a stress pulse, $\underline{\tau} = 108$ g/mm^2.

18. Dislocation displacement vs. distance from the free end of a copper crystal, $\underline{\tau} = 108$ g/mm^2.

a)

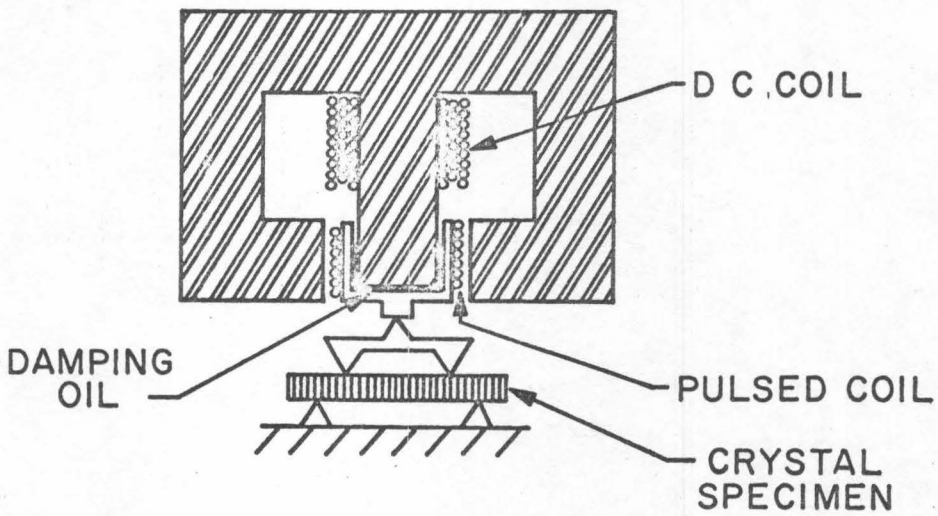
D C COIL
DAMPING OIL
PULSED COIL
CRYSTAL SPECIMEN

b)

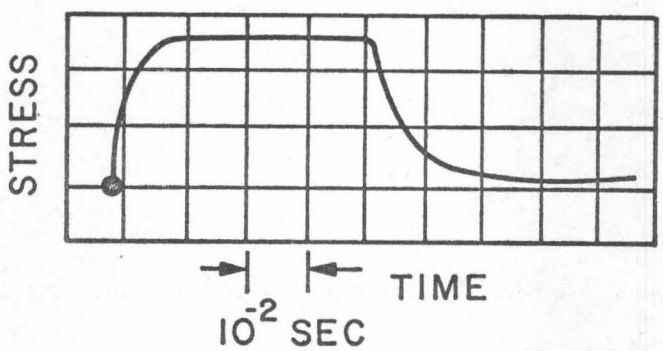
STRESS
TIME
10^{-2} SEC

FIG. 1

a)

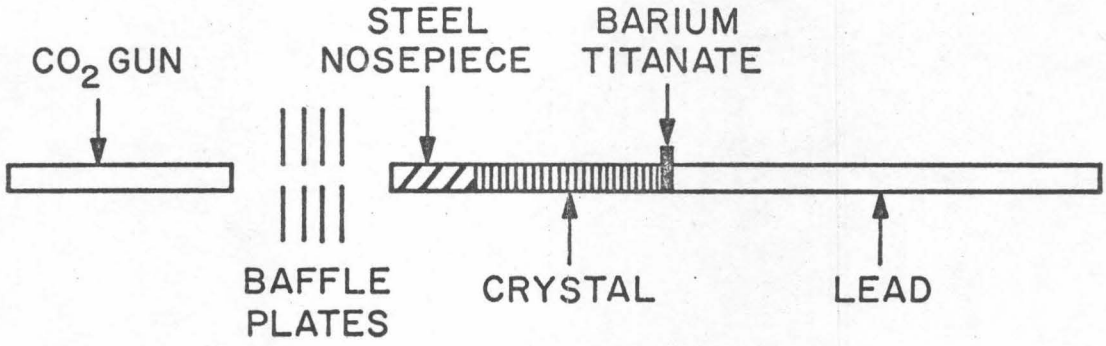
CO_2 GUN
STEEL NOSEPIECE
BARIUM TITANATE
BAFFLE PLATES
CRYSTAL
LEAD

b)

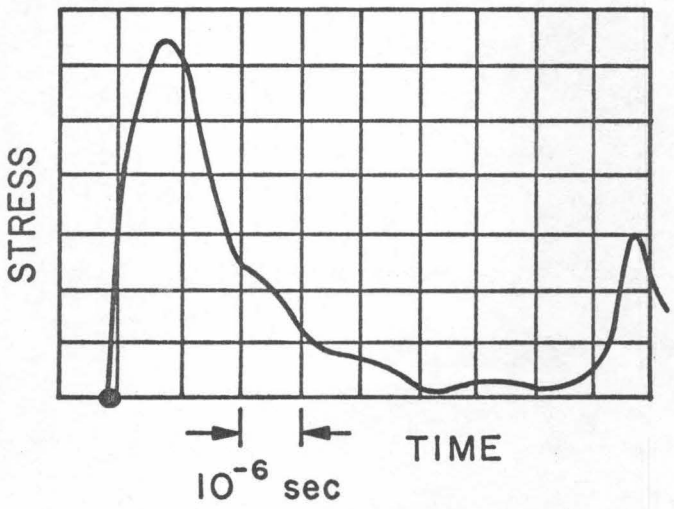
STRESS
TIME
10^{-6} sec

FIG. 2

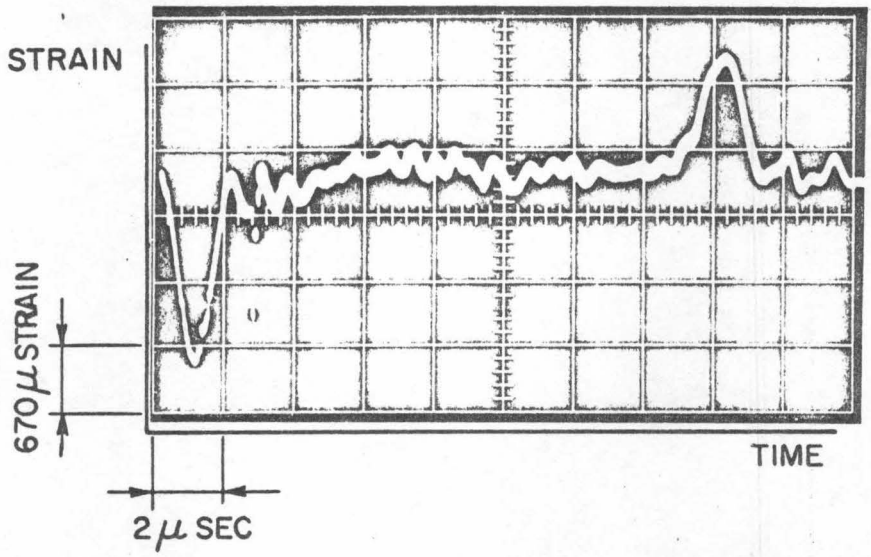

(a)

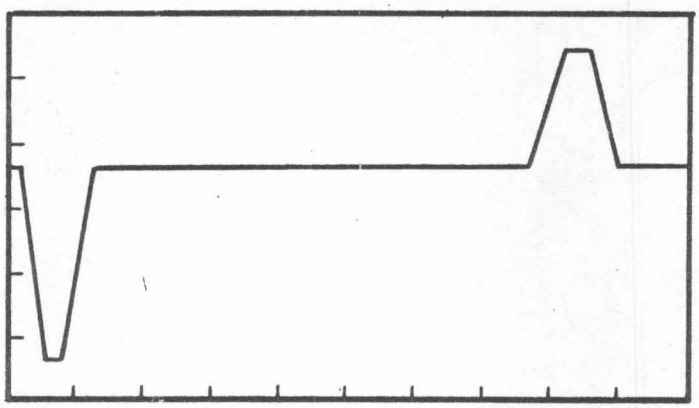

(b)

FIG. 4

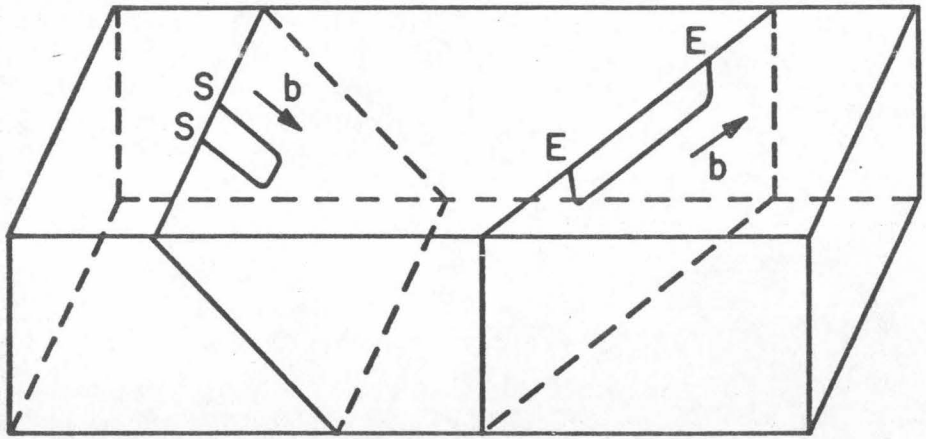

CLEAVAGE PLANE $\{100\}$
GLIDE PLANE $\{110\}$
GLIDE DIRECTION $\langle 1\bar{1}0 \rangle$

FIG. 5

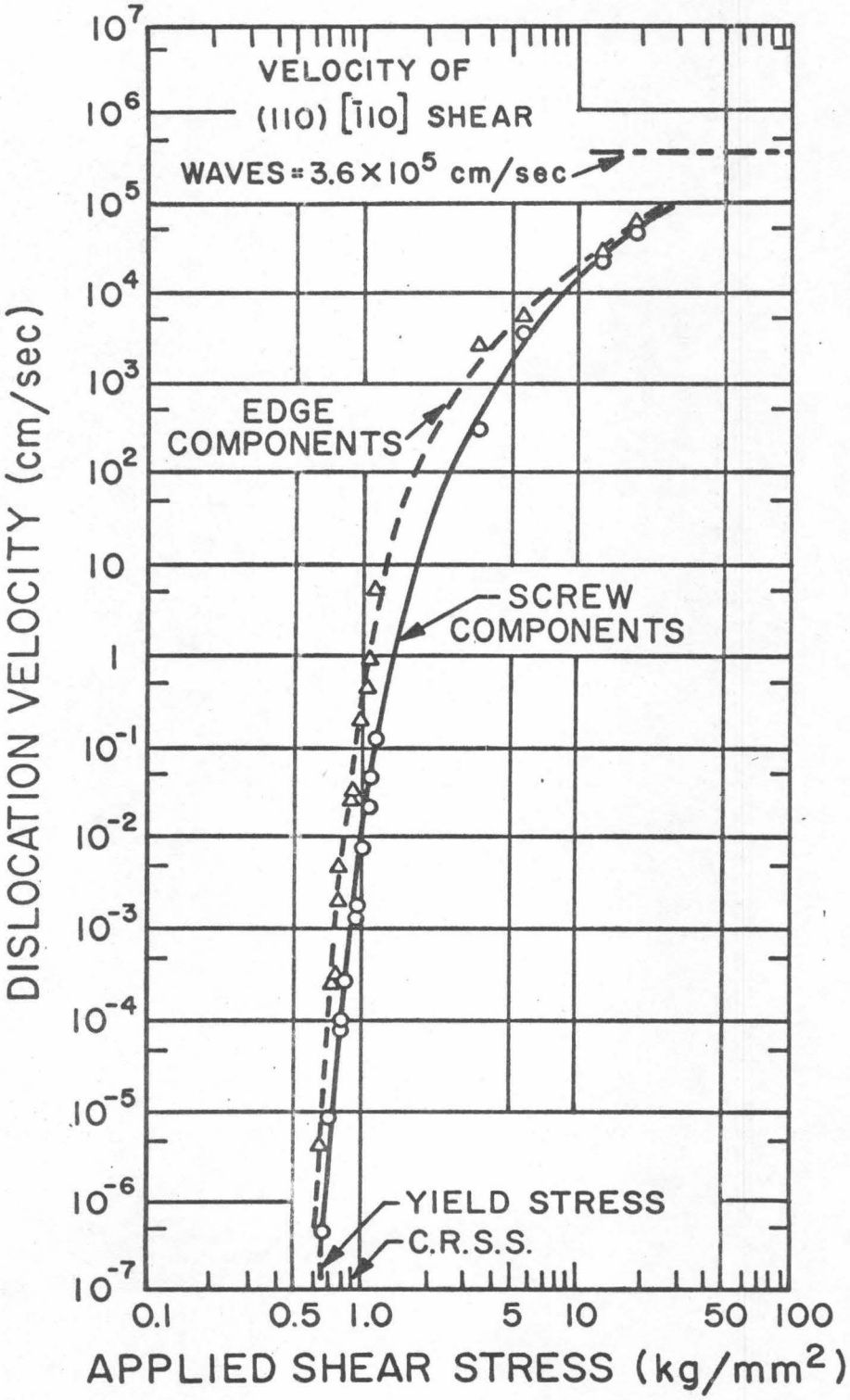
VELOCITY OF
(110) [$\bar{1}$10] SHEAR
WAVES = 3.6×10^5 cm/sec
EDGE
COMPONENTS
SCREW
COMPONENTS
YIELD STRESS
C.R.S.S.
DISLOCATION VELOCITY (cm/sec)
APPLIED SHEAR STRESS (kg/mm^2)
10^7
10^6
10^5
10^4
10^3
10^2
10
1
10^{-1}
10^{-2}
10^{-3}
10^{-4}
10^{-5}
10^{-6}
10^{-7}
0.1
0.5
1.0
5
10
50
100

FIG. 6

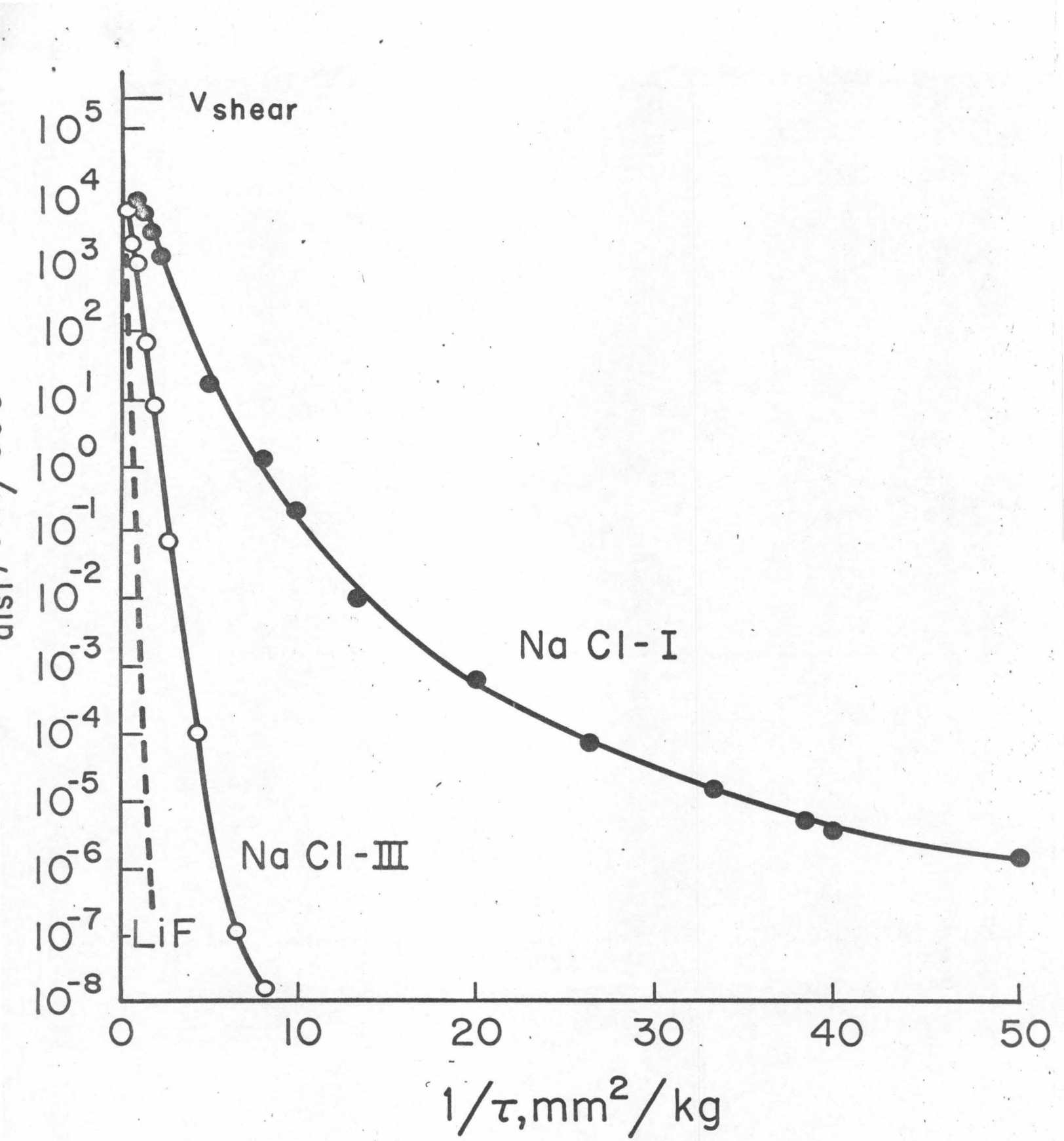
v_{shear}
10^5
10^4
10^3
10^2
10^1
10^0
10^{-1}
10^{-2}
10^{-3}
10^{-4}
10^{-5}
10^{-6}
10^{-7}
10^{-8}
Na Cl - I
Na Cl - III
LiF
0
10
20
30
40
50
$1/\tau, mm^2/kg$

FIG. 7

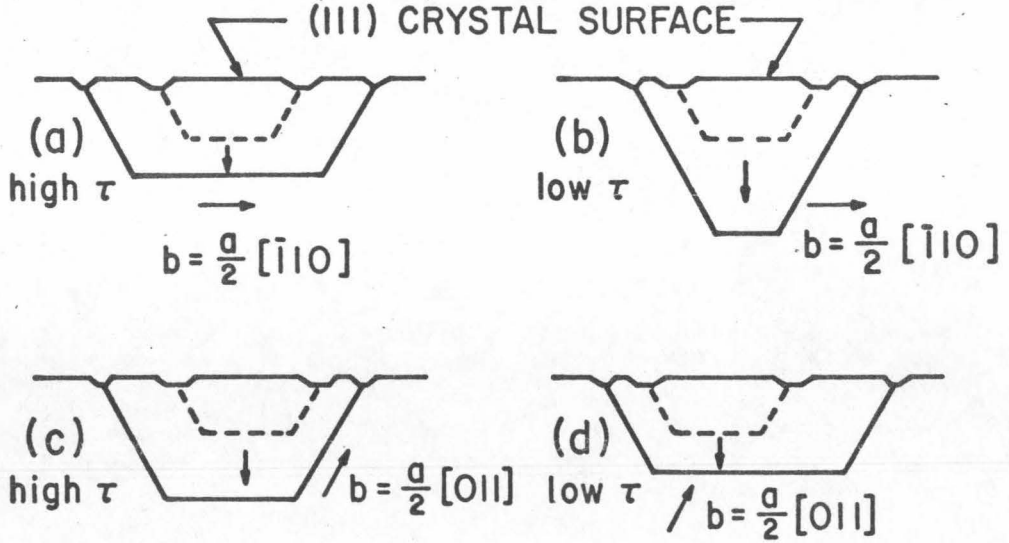
(111) CRYSTAL SURFACE
(a)
high τ
b = a/2 [1̄10]
(b)
low τ
b = a/2 [1̄10]
(c)
high τ
b = a/2 [011]
(d)
low τ
b = a/2 [011]

FIG. 8

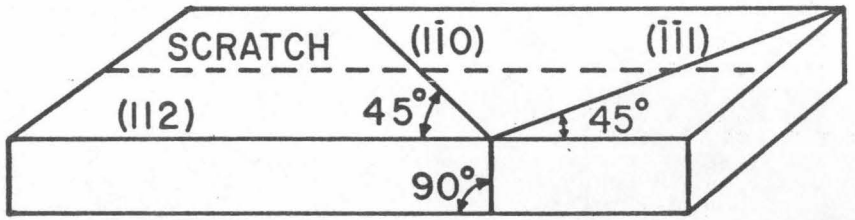

FIG. 9

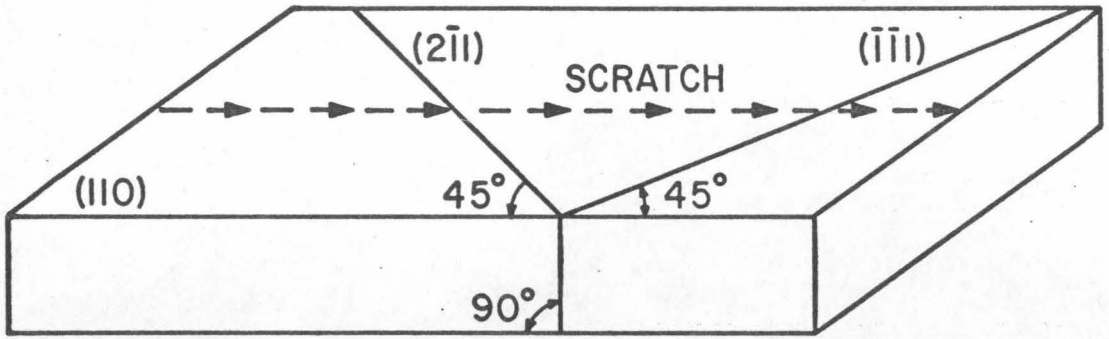

FIG. 10

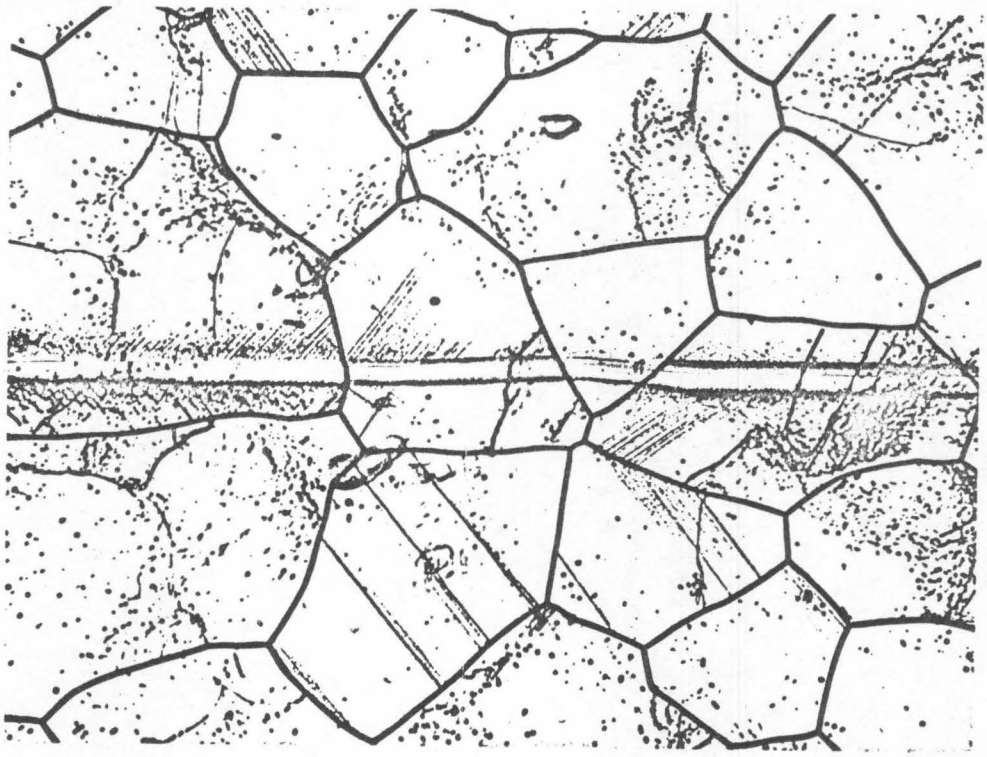

FIG. 11

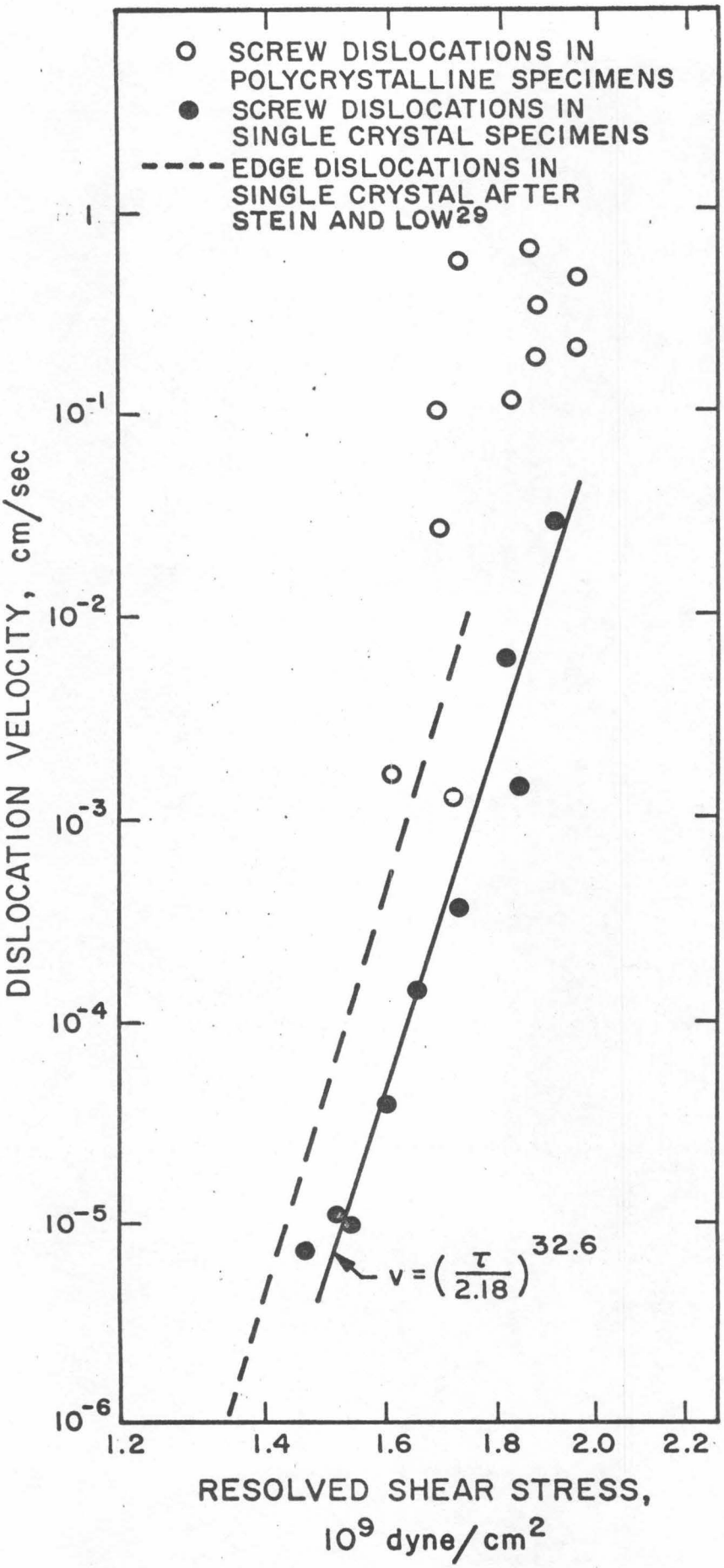
SCREW DISLOCATIONS IN POLYCRYSTALLINE SPECIMENS
SCREW DISLOCATIONS IN SINGLE CRYSTAL SPECIMENS
EDGE DISLOCATIONS IN SINGLE CRYSTAL AFTER STEIN AND LOW[29]
DISLOCATION VELOCITY, cm/sec
1
10^{-1}
10^{-2}
10^{-3}
10^{-4}
10^{-5}
10^{-6}
$v = \left(\frac{\tau}{2.18}\right)^{32.6}$
1.2
1.4
1.6
1.8
2.0
2.2
RESOLVED SHEAR STRESS,
10^9 dyne/cm^2

FIG. 12

a)

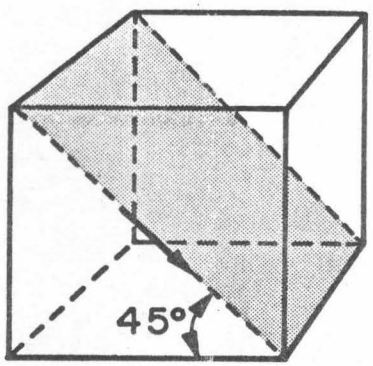

FRONT $(10\bar{1}0)$

(0001) $[\bar{1}2\bar{1}0]$

b)

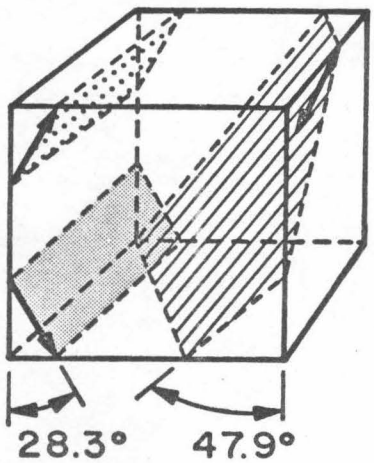

FRONT $(10\bar{1}0)$

TOP (0001)

SIDES $(\bar{1}2\bar{1}0)$

$(\bar{1}2\bar{1}2)$ $[1\bar{2}13]$

$(\bar{2}112)$ $[2\bar{1}\bar{1}3]$

$(1\bar{2}12)$ $[\bar{1}2\bar{1}3]$

c)

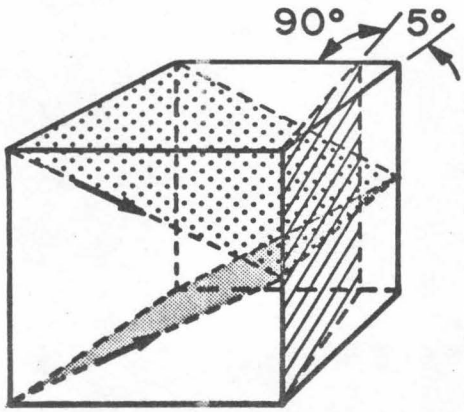

FRONT $(10\bar{1}0)$

TOP $(1\bar{2}10)$

SIDES $(\bar{1}01\ 24)$

$(1\bar{2}12)$ $[\bar{1}2\bar{1}3]$

$(\bar{1}2\bar{1}2)$ $[1\bar{2}13]$

(0001)

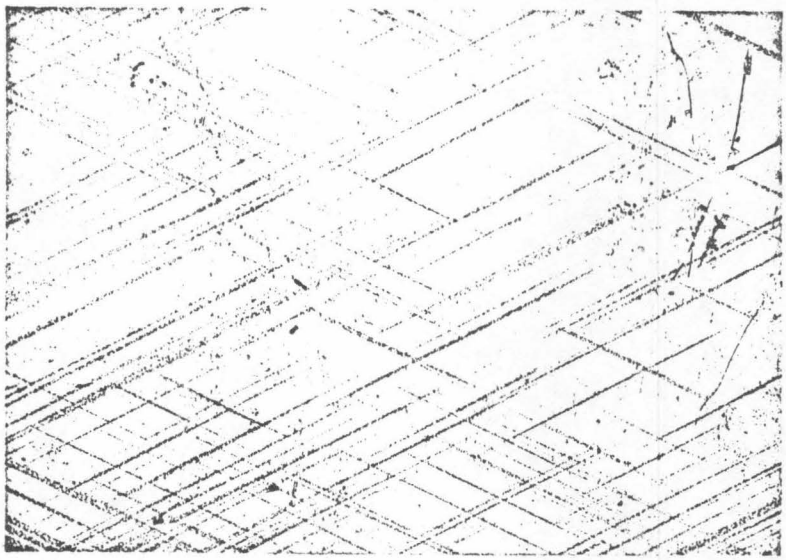

(a)

0.1 in.

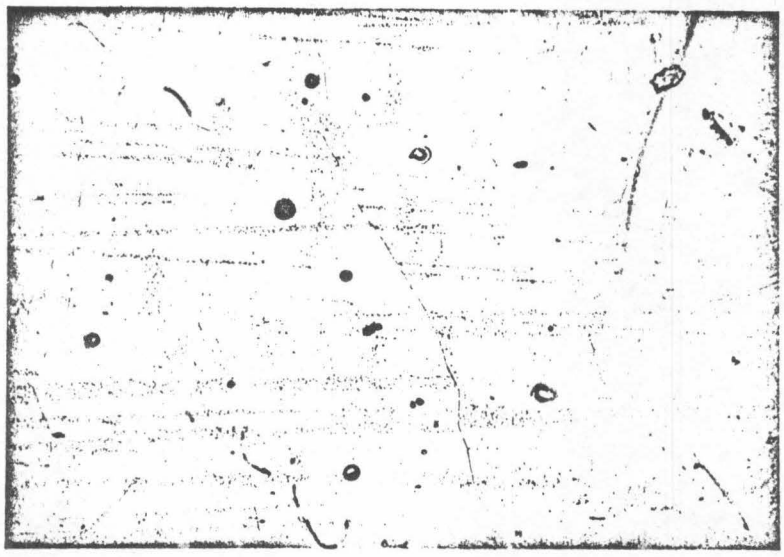

(b)

FIG. 14

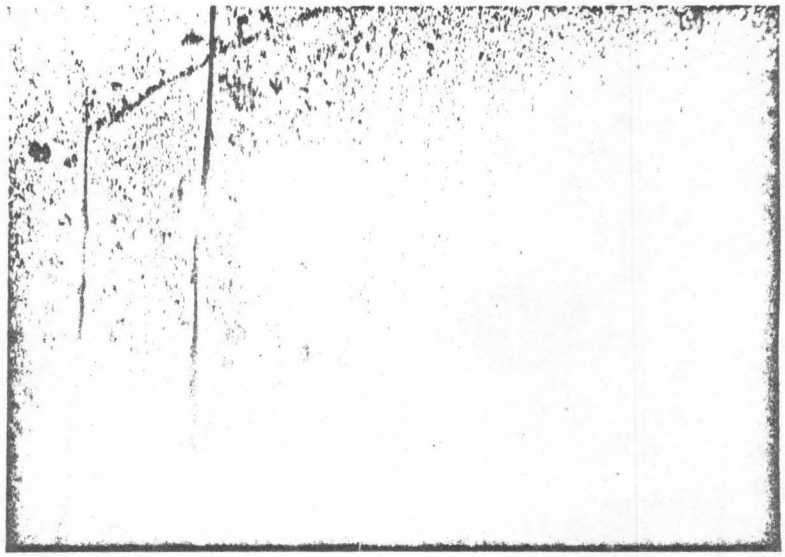

(a)

$[1\bar{2}10]$ 0.01 in.

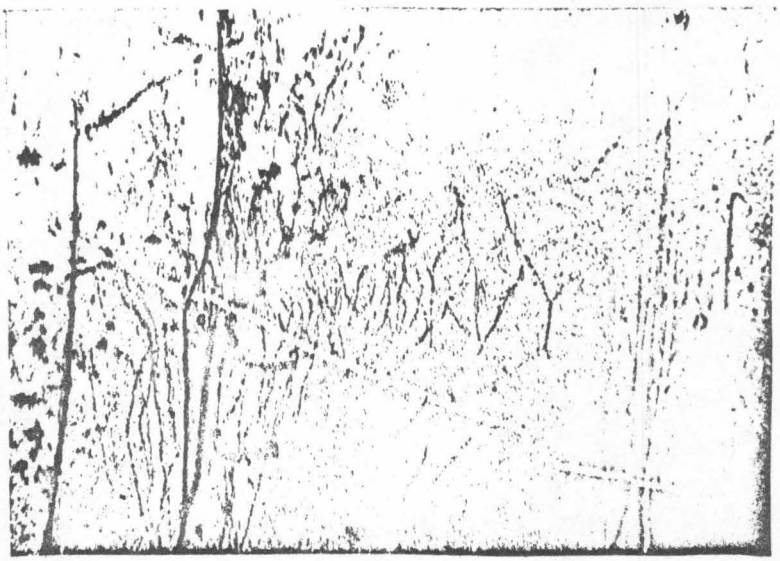

(b)

FIG. 15

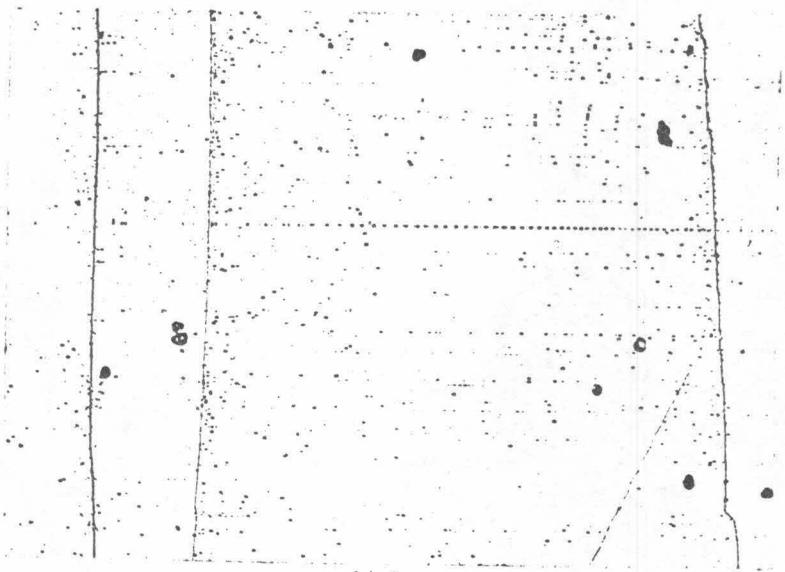

(a)

$[1\bar{2}10]$

0.01 in.

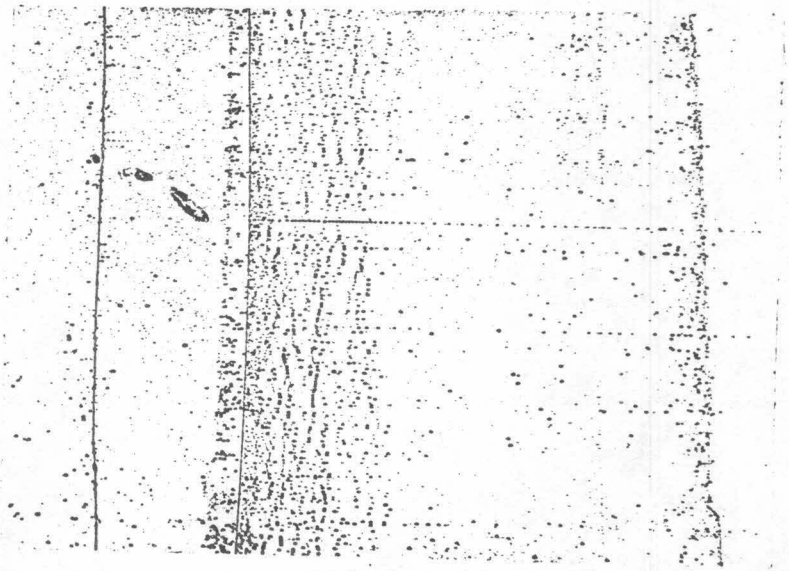

(b)

FIG. 16

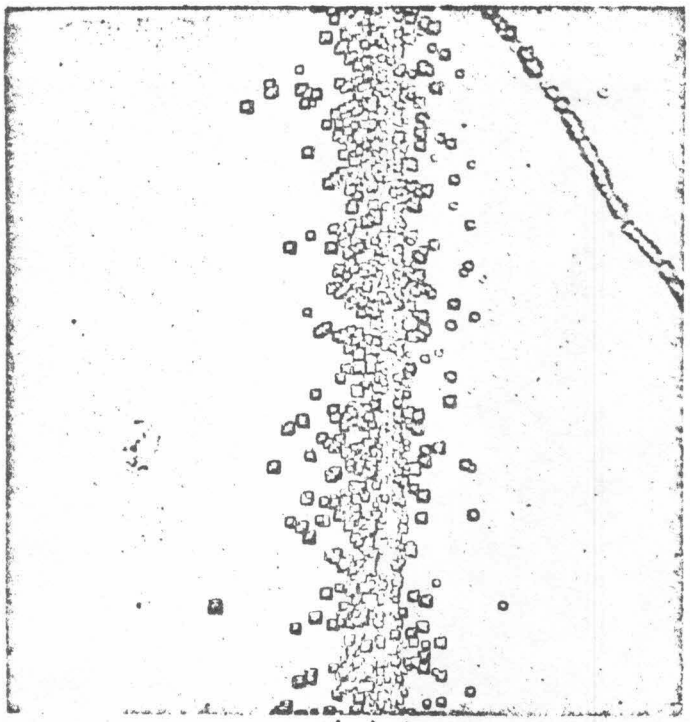

(a)

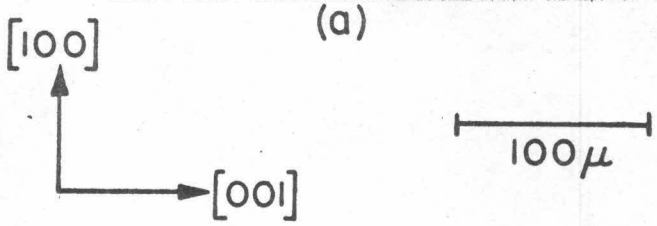

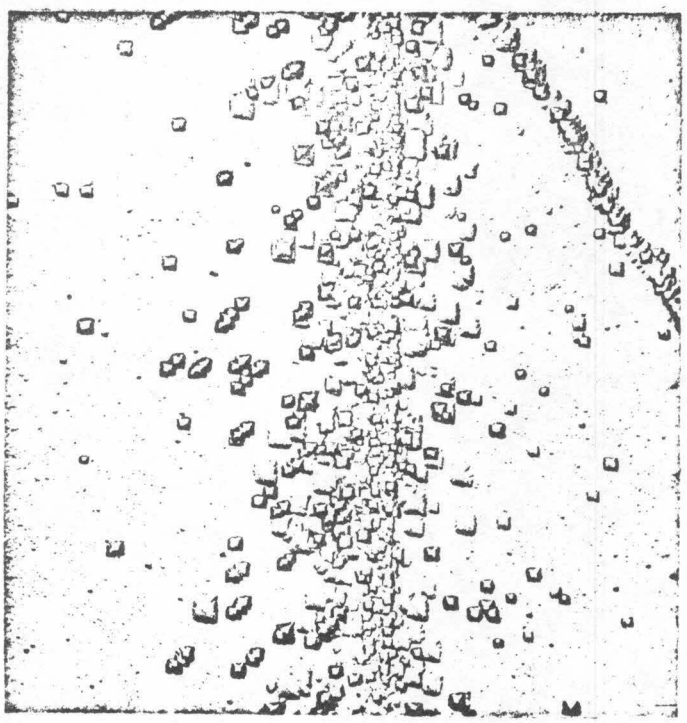

(b)

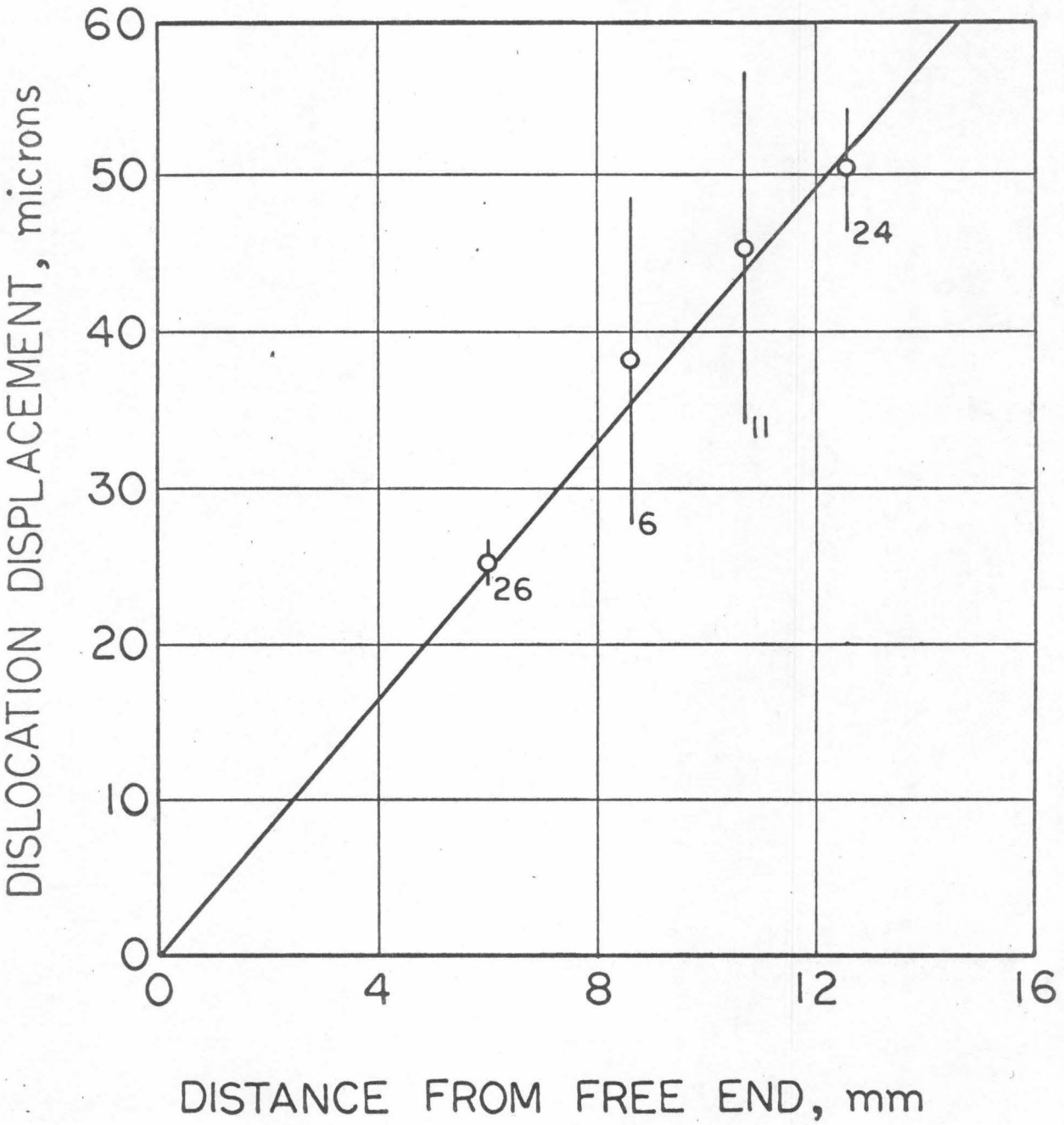
DISLOCATION DISPLACEMENT, microns
60
50
40
30
20
10
0
0
4
8
12
16
DISTANCE FROM FREE END, mm
26
6
11
24

FIG. 18